ADDIS ABABA UNIVERSITY

ADDIS ABABA INSTITUT OF TECHNOLOGY

SCHOOL OF MECHANICAL AND INDUSTRIAL ENGINEERING

GRADUATE PROGRAM IN RAILWAY ENGINEERING

FATIGUE ANALYSIS OF THE RAIL FASTENING E-CLAMP ON AA-LRT

A THESIS SUBMITTED TO THE SCHOOL OF MECHANICAL & INDUSTRIAL RAILWAY STREAM

BY:

NAME: HOUMED WALINO KADRI

ID/N: GSR/3201/06

ADVISOR:

DR DANIEL TILAHUN

JUNE, 2016

DECLARATION

I here by declare that the work which is being presented in this thesis entitled ‘’**FATIGUE ANALYSIS OF the RAIL FASTENING E-CLAMP ON AA-LRT’’** ’ is original work of my own, has not been presented for a degree of any other university and all the resource materials used for this thesis have been duly acknowledged.

_____ _____

Houmed walino kadri Date

This thesis has been submitted for examination with my approval as a university advisor

_____ _____

Dr. Daniel Tilahun (Advisor) Date

ADDIS ABABA UNIVERSITY
ADDIS ABABA UNIVERSITY INSTITUTE OF TECHNOLOGY
SCHOOL OF MECHANICAL AND INDUSTRIAL ENGINEERING

‘’FATIGUE ANALYSIS of the RAIL FASTENING E-CLAMP ON AA-LRT’’

By

HOUMED WALINO KADRI

Approved by Board of Examining

Dr. Birhanu Beshah Railway Center Head	_____ Signature	_____ Date
Dr. Daniel Tilahun Advisor	_____ Signature	_____ Date
Ato Araya A. (PhD candidate) _____ Internal Examiner	_____ Signature	_____ Date
Ato Hailelul (PhD candidate) _____ External Examiner	_____ Signature	_____ Date

ABSTRACT

The goal of this study is analyzing and identifying the stresses on E-clamp due to the wheel load to predict and minimize failures caused. This study covers the stress and failure caused by the wheel load. Under normal track and load conditions, E-clamp fail due to high cycle fatigue.
The 3D model has done on modeling package of CATIAV5R19. In CATIAV5R19, different components of wheel/rail assembly i.e. wheel, rail, E-clamp, bolt, nuts, rail pad are created separately then all components are assembled, and create a complete model of wheel/rail assembly. Assembly model has created in assemble workbench of CATIA after individual component of joint had created on part work bench.

After the assembly is accomplished on CATIA, it was imported in to the ANSYS v14.0 to analyze the stress caused by vertical load. The meshing type for this research is medium size meshing. All the material properties are being applied. During the analysis of wheel/rail contact in ANSYS software, the parameters have been used wheel load angular and simulation result is obtained.

The analysis includes fatigue stress von miss stresses, shear stress and Equivalent elastic strain and fatigue life. These values have been determined under the influence of wheel load. The result obtained in this analysis is less and better stress values for E-clamp by the modified geometry. This paper recommends that during the analysis of E-clamp that the new geometry E-clamp is better than the existing. For the similar problem engineers can develop the solutions by modification of the geometry of rail fastening component parts.

Key Words: Rail fastening, Modeling, Finite Element

ACKNOWLEDGEMENTS

First I would like to express my heart felt appreciation and gratitude to my advisor Dr Daniel for his helpful advice and for the faith, guidance, and help that he gave to me during my project work to be completed. I would also like to thank him for giving me the idea to take the project and "run with it" which allowed me to enjoy the project that much more. Without these ideas, this project would not have been the success that it has become and he deserves the credit for originating the concepts.

I would like to thank all those individuals at Addis Ababa University who have Supported me throughout my time as a post graduate student. I would like to thank Ato Sitataw for his helpful on Catia software and Ato Behailu PhD candidate.

I would also like to thank my classmates for their support, direction, and wonderful explanations to help me further understand the basics of my research; and for their many recommendations and always helping me in idea as well as how to use the software's that helped me in doing the research.

I would also like to express my gratitude to friends in Ethiopian Railway Corporation, who provided their vast knowledge of railroad design to help me complete this research.

Table of content

List of Table

LIST of FIGURE

NOMENCLATURE

a: Minor semi axes of the contact ellipse

b: Major semi axes of the contact ellipse

F: Vertical load, JBG:joint bar geometry

m & n :Hertz coefficients

Kw: Constants that depend on the material properties of railway wheel

ν_w: Poisson's ratio wheel material

E_w: Young's modulus of the railway wheel material

ν_r: Poisson's ratio of rail material

E_r: Young's modulus of rail material

R_{1w}: Principal rolling radii of the wheel

R_{1r}: Principal rolling radii of rail

R_{2w}: Principal transverese radii of curvature of wheel

R_{2r}: Principal transverese radii of curvature of radii

K : Stiffness matrix of the system

U: Nodal displacement vector

Γ_1: Boundary with zero displacement,

Γ_2: Boundary where measured displacements are given

Γ_3: Boundary with unknown contact forces F_c

Γ_4: Boundary where there are known applied forces

F_a: Applied forces

U_1: Displacements on constrained boundary Γ_1

U_2: Known and measured displacements on free boundary Γ_2

U_3: Unknown displacements on contact boundary Γ_3

CHAPTER ONE

1. INTRODUCTION

1.1. Background

A modern steel rail has a flat bottom and its cross section is derived from I -profile. The upper flanges of the I-profile have been converted to form the railhead. Recently the common used rail profile is the UIC60 rail, where 60 refer to the mass of the rail in kg per meter. The rails provide continuous and level surface for movement of trains. The rails provide a pathway which is smooth and has very less friction. The rails serve as a lateral guide for the running of wheels. The rails bear the stresses developed due to vertical loads transmitted to it through axles and wheels of rolling stock as well as due to braking forces and thermal stresses.

The rails carry out the function of transmitting the load to a large area of formulation through sleeper's ballast. The rails also act as electrical conductors for signaling system [3]. However, Ethiopia LRT is use the GB 50kg/m rail. A track structure consists of rails, sleepers, rail pads, fastenings, ballast, sub ballast, and sub grade, see the figure below. Two subsystems of a ballasted track structure can be distinguished: the superstructure composed of rails, sleepers, ballast and sub ballast, and the substructure composed of a formation layer and the ground. [4] Rail is the most important track element subjected to wheel loads must be able to securely sustain these loads applied in vertical, lateral, and longitudinal directions and subsequently transfer them to the underlying supports. Rail is the track element, which is direct contact with the rolling stock. It is therefore very necessary, in particular from a safety point of view, to ensure the proper functioning of rails in the track system.

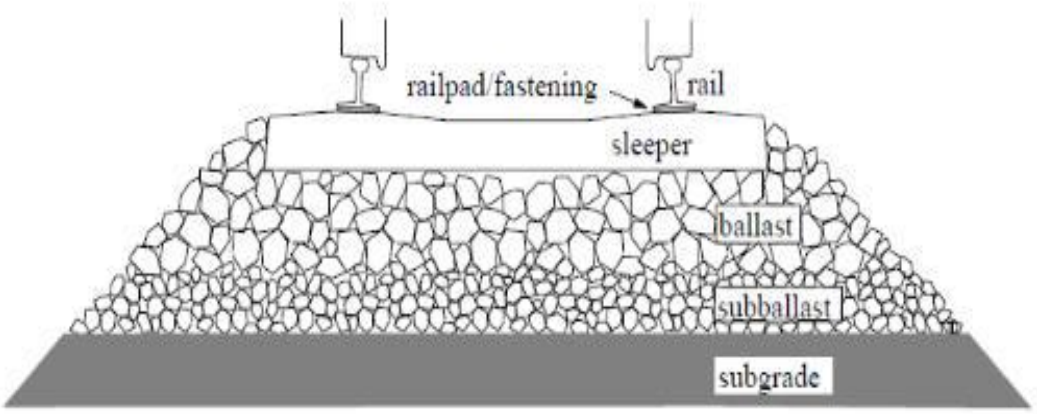

Figure1.1: Track with different components. [3]

1.2 Railway Track components overview

Railroad track is known a stable structure that mainly consists of rail sleepers, fishplates and fasteners. It ensures the transportation of trains through providing a dependable surface for their wheels [4]. In different countries, railway track components have different names, such as in UK and UIC terminology, it is often referred to as railway track, while railroad track is used predominantly in the US. As to the development of railway track, it has a long history [5]. The first rail track was made of wood and continued for about 50 years. Later, in order to reduce the wear of the wooden rail tracks, iron straps were mostly added to the wooden rails. Then it was followed and widely used by cast iron rails. And in recent days, steel rails are mainly rolled in a continuous casting process. Over the years, the shape of rails has changed a lot. Since first rolled in 1831, the "T" section has been the standard in North America. [10]

1.2.1Railroad sleepers

Sleepers play important roles in railway track system [7]. The primary function of the sleepers is to transfer the vertical, lateral and longitudinal rail seat loads to the ballast, subballast and subgrade layers. They also serve to maintain track gauge and alignment by providing a stable support for the rail fasteners [7-8].Rail sleepers are an important part of railway components. In general, they are also called railroad ties, railway ties or crossties. In order to keep the correct distance of gauge, the rail sleeper usually lays between the two rail tracks.

Figure 1.2 Standard rails fastening of Addis Ababa LRT.

For more than one hundred years, the railroad ties have been developed to meet the various requirements of the different railway tracks. With the development of steel tracks, steel sleepers appeared and were common in the UK. Later, between the line Nuremberg and Bamberg in Germany in 1906, the concrete sleeper occurred. In the recent time, concrete sleepers are widely used in the transportation of rail tracks especially in Europe and Asia. Besides, there are still some special types of railroad sleepers such as plastic composite ties which are also employed in the rail track transportation [8].

1.2.2 Rail fastenings

The fastening system, or "fastenings," includes every component that connects the rail to the sleeper. Fastenings clamp the rail gauge within acceptable tolerances and then absorb forces from the rails and transfer them to the sleepers. Vibration and impact from various sources e.g. traffics, natural hazards, etc. are also dampened and decelerated by fastenings. Fastenings sometimes act as electrical insulation between the rail and the sleepers. Their primary components are fastener and rail pad. Some tracks might have base plates with or without pads, which helps the workmen to remove damaged rails without having to untie the fastenings and immediately replace them with new rails. In this case the rail is only connected to the immediate base plate. This system is called indirect fastenings which differ from the usual direct fastenings in that the latter device is built-in and holds the rail directly onto the sleepers.

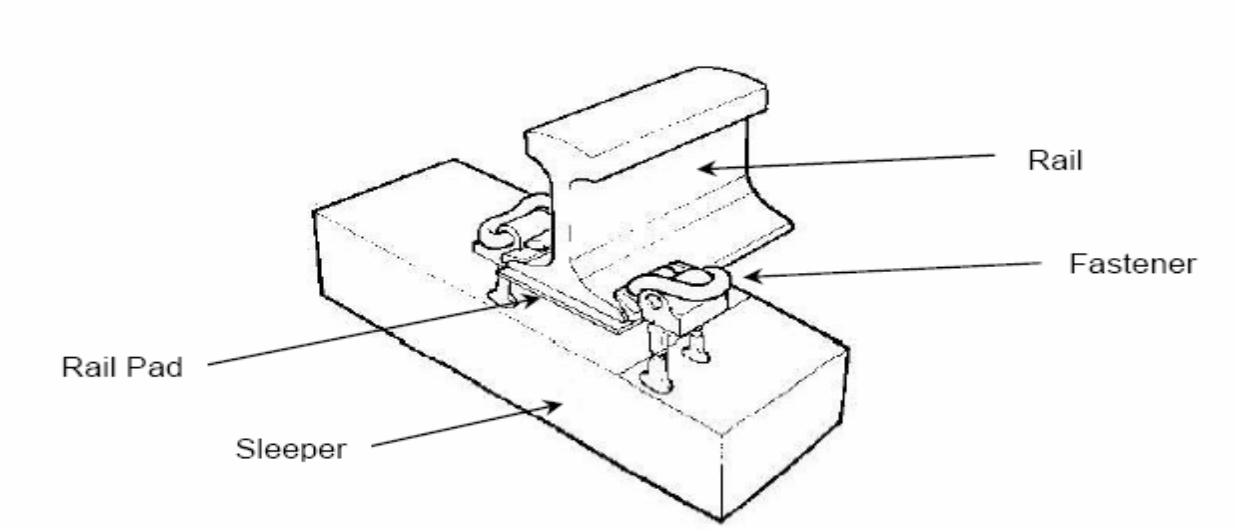

Figure1.3 A typical concrete fastening system.

1.2.2.1 Rail fastener

Because there are many different types of fasteners, their application depends on the characteristics, patterns, and structure of the sleepers to be used. The fasteners withstand the vertical, lateral, and longitudinal forces, and overturning moments of the track, as well as keeping the rails in place. They also transfer all the forces caused by the wheels, thermal change, and natural hazards, from the rails to the adjacent sleepers. Rail fasteners also known as fastening systems are used in railway track structure to fasten the rails to the sleepers and to protect the rail from inadmissible vertical, lateral, and longitudinal movements [9]. Moreover, these components serve as tools for gauge restraining, wheel load impact attenuation, increasing track elasticity, etc. There are various types of rail fasteners which mainly are classified from two points of view as presented in Figure 1.4 [9]

.

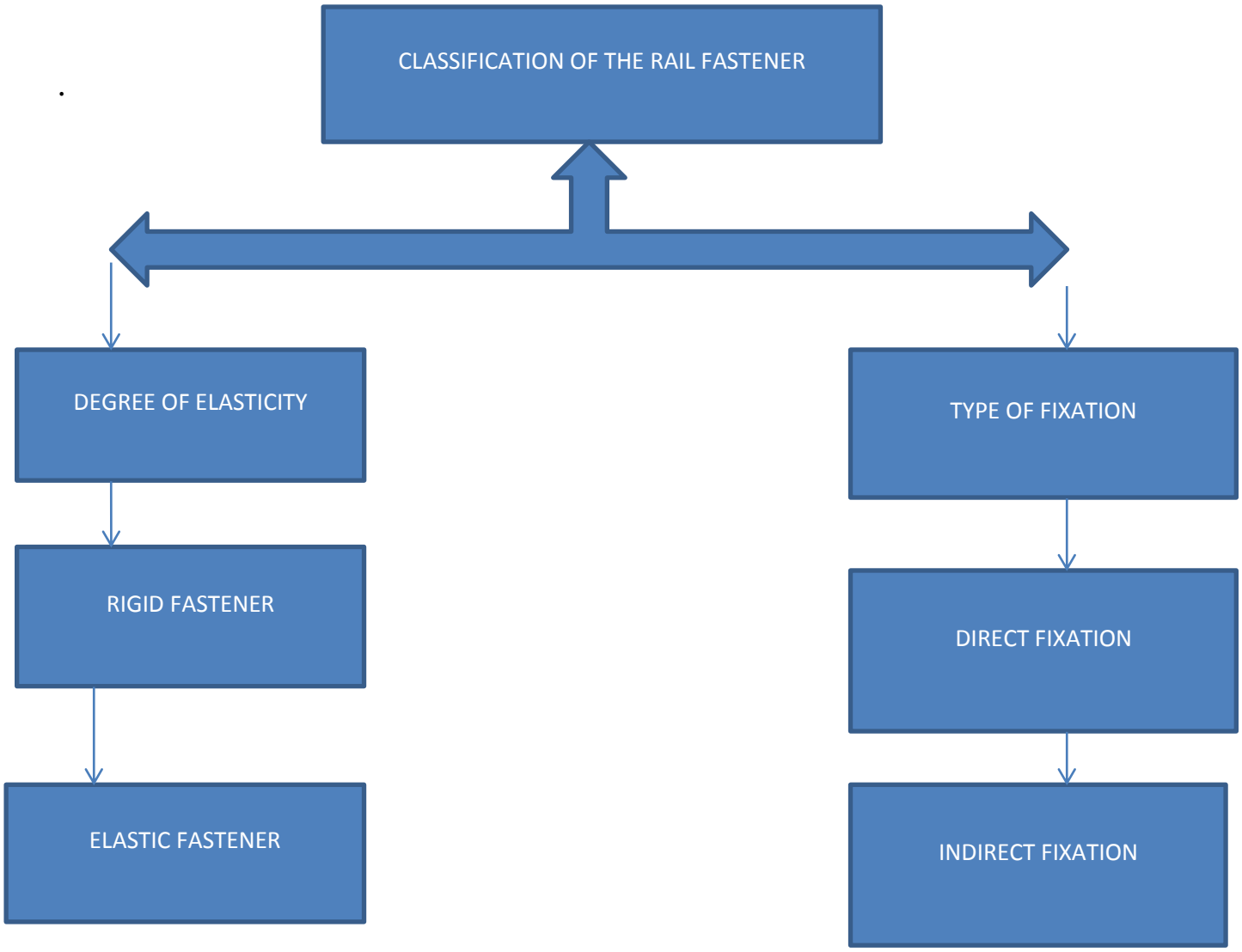

Figure1.4. Classification of the rail fastener

Among the components of rail track, the railroad fasteners are an important part. It can ensure the operation of rail transportation through connecting track rails with rail ties and rail sleepers. And it is also used to fix the correct position of tracks to prevent the horizontal and vertical displacement as well as the rollover. What's more, the good elasticity and insulating property also help rail fasteners do well in gauge adjusting.

In the current time, there are various types of railway fasteners in the global market, such as some widely and mainly used railway fasteners: VOSSLOH W type in Germany, FAST CLIP in UK, STEDEF NABLA fastener, PANDROL E type fastener, PR type fastener, and RN fastener

in France. They are assembled with other components as independent units, which can be fixed as a whole and can also offer under controlled vertical, longitudinal, and transverse forces to avoid excessive displacement.

Figure 1.5 Pandrol's clip fastening

Figure1.6 Tension clamp fastening

1.2.2.2 Rail Pads

Rail pads are placed on the rail seat to filter and transfer the dynamic forces from rails and fasteners to the sleepers. The high dashpot value of rail pads reduces excessive high-frequency forces and provides a resiliency between rail and sleeper that helps alleviate rail seat cracking and contact attrition.

1.2.2.3 Sleepers

Sleepers are transverse beams resting on ballast and support. Wooden sleepers were used in the paste because timber was readily available in the local area. However, pre-stressed or reinforced concrete sleepers, and to a limited extent steel sleeper, have been adopted in modern railway tracks over the past decades because of their durability and long service life. [4] Grouped timber Sleepers into two types: softwood (e.g. pinewood) and hardwood (e.g. beech, oak, tropical tree). Concrete sleepers are described as either twin-block or mono-block [5]. Within all these types, concrete sleepers are more widely used because they are not affected very much by either climate or weather.

The important functions of sleepers are:

- To uniformly transfer and distribute loads from the rail foot to the underlying ballast bed;
- To provide an anchorage for the fastening system that holds the rails at their correct gauge and preserves inclination, and
- To support the rail and restrain longitudinal, lateral and vertical movement by embedding itself onto the substructures.

Figure 1.1.2.3 Types of concrete sleepers

1.3. History of the rail fastening

The earliest wooden rails were fixed to wooden ties by pegs through holes in the rail, or by nails. By the 18th century cast iron rails had come into use, and also had holes in the rail itself to allow them to be fixed to a support.18th century developments such as the flanged rail and fish bellied rail also had holes in the rail itself; when stone block ties were used the nails were driven into a wooden block which had been inserted into a recess in the block. The first chair for a rail is thought to have been introduced in 1797 which attached to the rail on the vertical web via bolts.

Figure 1.6 Rail to wooden sleeper fitting

By the 1820s the first shaped rolled rails had begun to be produced initially of a T shape which required a chair to hold them; the rails were held in position by iron wedges (which sometimes caused the rail to break when forced in) and later by wooden wedges, which became the standard. In the 1830s Robert L. Stevens invented the flanged 'tee' rail (actually a distorted I beam), which had a flat bottom and required no chair; a similar design was the contemporary bridge rail (of inverted U section with a bottom flange and laid on longitudinal ties); these rails were initially nailed directly to the tie.

In North American practice the flanged T rail became the standard, later being used with tie-plates. Elsewhere T rails were replaced by bull head rails of a rounded 'I' or 'figure-8' appearance which still required a supporting chair. Eventually the flanged T rail became commonplace on all the world's railways, though differences in the fixing system still exist.

Figure1.7. Rail spike with baseplate above the tie

1.4 Statement of the Problem

Fastenings are all the materials whose function is to structurally connect the rail to the sleeper. The fastenings used in concrete sleepers must be resilient, presenting elasticity in both tension and compression, upwards and downwards. The basic component of all types of fastenings consists of an elastic steel rod or plate, named fastening's clip, or fastening's plate, that are springs. Spring clip normally provide a flexible connection between the rail and the sleeper. They also provide a mitigation to suppress the vibration created by the traffic impact. One pair of clips per rail, acting on the upper part of the rail foot, together with one "compatible" resilient pad, underneath the rail's seating surface, function as one ensemble. The pad provides elasticity (springs) under the rail's seating surface (Fig. 2), it is produced from elastic material and it must be compatible to the clip.

By their very nature, rail fastening E-clamp creates discontinuities in the running surface of the rails. In addition to bending, residual stresses, rail fastening are also subjected to static load due to these discontinuities. Under normal track and load conditions, E-clamp fail due to high cycle fatigue. Accelerated track degradation increases deflections, which further increase E-clamp stresses. Rail fastening E-clamp failures are a safety and reliability concern for railroads.

The stresses on the rail head produce the deflection on the rail fastening E-clamp that causes to vary on the rail and e-clamp profile. As the result, the profile of rail fastening component change from its normal profile it originates the discomfort and safety problem to the passenger and accident on the vehicle by causing wear on fastening part identification and improving of the stresses on the rail fastening assist to increase maintenance period for rail fastening, to reduce

and avoid the discomfort of the passenger, rail fastening wear and its maintenance cost by using of different mechanism to decrease the fatigue stress on rail fastening component.

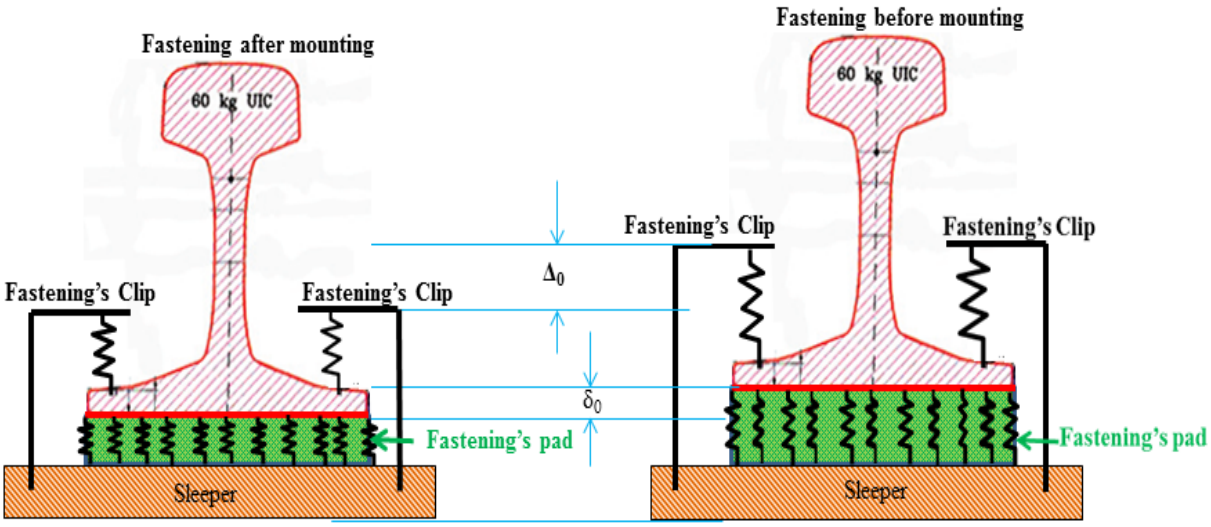

Figure 2: Fastening in schematic depiction, before mounting (right illustration) and after mounting (left illustration)

1.5 Objectives of the study

1.5.1 General Objective:

The main objective of this study is analyzing and improving the stresses on E-clamp due to the wheel load, which cause failure.

1.5.2 Specific Objective:

- improving the existing E-clamp in order to reduce the von miss stresses caused by wheel load
- Reduce the maximum deformation on the E-clamp.
- Reduce fatigue stresses on E-clamp.
- Fatigue life of E-clamp

1.6 Methodology of the research

- ✓ The 3D model has done on modeling package of CATIA v5R19:
  - First on CATIA modeling different components of rail fastening system and assembly ie.

- Rail, sleeper, fastening screw,
- Rail clamp ,rail pad ,
- Angle guide plat
- After the assembly is accomplished on CATIA, it is imported to the ANSYS v14.5. The analysis carries out to determine the stress distribution over the construction.

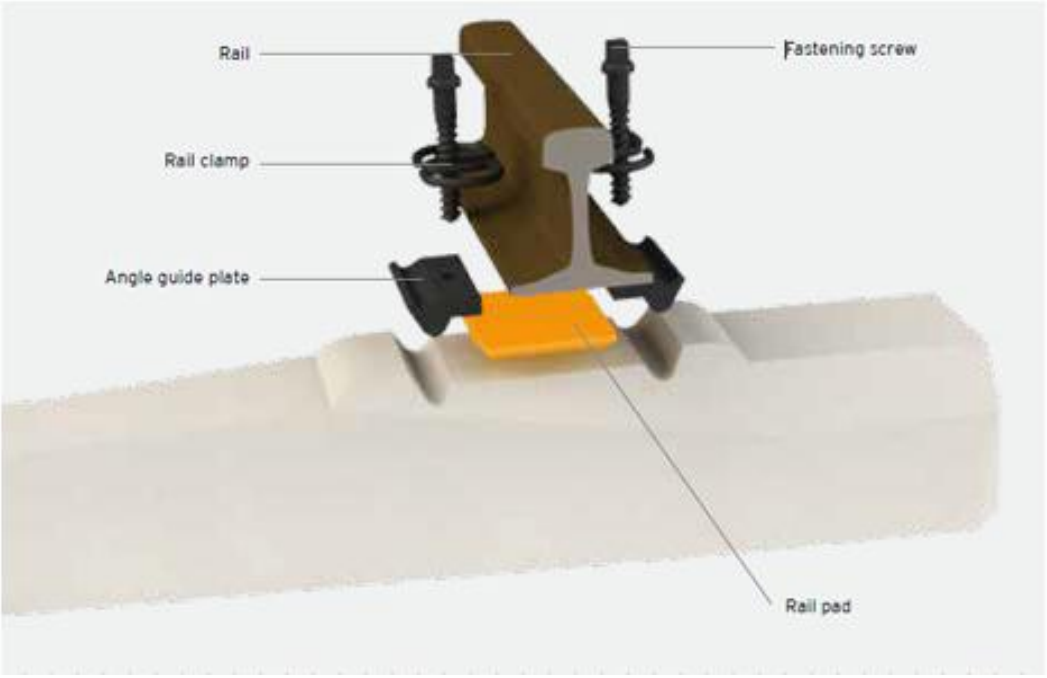

Figure3: Typical figure of the rail fastening system

1.7 Significance of the research

This research has a great role for future analysis and uses of rail fastening, in general for newly constructing Ethiopian railway by studying the new geometry of rail fastening E- clamp. In the future, it will add new knowledge about existing one with analysis of rail fastening E-CLAMP stress, strain, deflection under vertical wheel load, which cause wear, fracture and deteriorations of the rail. This paper try to figure out those problems related to the rail fastening due to the wheel loading between the sleeper supports based on engineering mechanics.

1.8 General Parameters and Conditions

1.8.1 General parameters

There are parameters to analyze the stress at the rail fastening between the sleeper concrete the rail on both sides. These parameters can be classified as follows:

- Vehicle parameters: operating speed, Empty vehicle, Seating capacity and overload capacity
- Track parameters: Rail and spring profile, tie space and rail fastening spring clip geometry (straight, location of rail between the tie).

1.8.2 General Conditions:

During the preparation of this paper the general conditions that have been using the effect of the wheel and rail contact at rail fastening. It is performed based on the Hertz contact theory. These are:

- The surface of contacting bodies is assumed smooth.
- The contact is assumed elastic.
- Isotropic and homogeneous material.

1.9 Scope and Limit of the Thesis

As it can be seen, numerous types of simulations can be carried out regarding to railway track fastening. In this research, as it is mentioned earlier, fatigue stress analysis of a rail fastening E-CLAMP structure are carried out. Nonlinear behavior which components could experience is not dealt with and, linear and isotropic material models are used for the entire analysis. The effect of friction is not taken into account when the analysis preformed. This study is to reduce stress to succeed the rail fastening. The limitations of the researches are lack of data, lack of high performance computer and lack of enough reference books to the research.

1.10 Organizations of the paper:

The body of this study is divided into five main chapters. The first chapter discusses background, objectives and methodology of the study. In addition, the details of the rail fastening type and rail fastening E-CLAMP used for analyze. The second chapter covers the review of some of the journal articles, conference papers and publications which were referred to during

the study. Also, in relation and comparison with previous works, what is done in this study will be stated. Analysis of stress on rail joint is discussed in the third chapter. Modeling contact at rail fastening, stress model using hertzian theory, rail support and wheel- rail simulation presented. In addition, it covers discretization of the solid model of the rail joint used for the analysis and load condition. The results obtained from the static and fatigue analysis of the rail fastening and discussions based on these results are included in the fourth chapter. Finally, the fifth chapter cover conclusions drawn based on the results of the analysis, recommendations and future work.

CHAPTER TWO

2. LITTERATURE REVIEW

2.1. Related Research

Fatigue life estimates can be used to guide the selection of inspection intervals for rail joint bars in service. A three -dimensional finite element model for rail Fastening is developed and

dynamic load is applied to estimate the fatigue life of the fastener E-clamp. Different components of the rail fastening system are being created separately and assemble in ABAQUS. The model consists of assembly of the rail, E-clamp, bolt, nut, washer, sleeper and Wheel. A three -dimensional finite Element analysis of rail fastening system and E-clamp are carried out in ANSYS after importing from ABAQUS. Create relatively complex and realistic three-dimensional structures that can be analyzed much more quickly and still provide reasonable results for studying the Effect of critical parameters. And puts some of the sections that describe the Methodology behind the creation of rail elements for use in a standard fastener Model utilizing shell elements. This was performed in order to investigate the Effectiveness of shells in modeling rail elements and to compare the results to the Investigations by.

In the study [1] investigated a standard E-clamp fastener configuration connecting Two sections of closed track .A Wheel load of 55574kg is applied on E-clamp Without curve and E-clamp with curve to see the difference and get the best. [3] Kantantinos Giannokos: studied the influences of the Secondary Stiffness of the clip on the behavior of the rail in the track panel in terms of the rail Tilt/ rotation, the clamping force, and rigidity. He concluded that the demands f or a modern Railway Track Fastening should be: (1) low static stiffness coefficient $\rho static<100$ kN/mm for the fastening as derived from the Load-Deflection curve of the pad, (2) Compatibility of the Clip and the Pad of the Fastening as it is derived from the combination and comparison of the Load-deflection Curves of the Clip and the Pad (toe-load in any case >8 kN), (3) Secondary stiffness in Order to decrease the "tilt of the rail" and keep it under a maximum limit of Approximately 2 mm. [4] ANALYSIS OF RAIL FASTENING SYSTEM DELTA LAGER I FAILURE: They Analyzed the possible caused for failure of rail fastening system DELTA LAGER I The type of fastening attributed as Delta Lager I is commonly used in underground

Railway system. Routine safety inspections revealed higher amount of broken high-strength steel bolts that secures interconnection between the rail and a Concrete sleeper. Performed computations were carried out using ANSYS 11.0 to help to found out cause of the problem. Spatial computational model of fastening Construction including different contact regions was modeled in conformity with drawing documentation. Further were performed non-linear computations in several alternatives of imperfections configuration. On accounts of FEM Computations were determined inadequacies in construction of rail fastening System. Bolts are

tightened by torque wrench to achieve the required 200 Nm of torque (Normal force in bolt is 126 KN). The second load case is vertical load caused by the locomotive (appropriate wheel force is 65 KN). Stress analysis of fastening was carried out for two possible conditions of initial geometry. In the first case the geometry of fastening is modeled strictly according to project

Documentation. Gap between the PE plates, which is laid under the steel Cantilever and solid sleeper, is included in computation model. In conformity with Documentation the gap is 3 mm. Finalizations of bolts in direction towards the Sleeper about 3 mm was carried out. Achieved normal force in bolt is 26 KN Abnormal rise of bending stress was noticed. [3] Numerical analysis of nonlinear Properties of rail fastening systems: Used tests on rail fastening systems and Simulation, the quasi-static test on rail fastening systems was carried out to Determine the quasi-static stiffness of the two Fastening specimens and to obtain The preload dependent nonlinearities. A shear type and a bonded compressed type Rail fastening systems are designed and produced for studying their different Preload dependent nonlinear mechanical behavior. Both of the two specimens were kept in a temperature of around 23 degree for two days prior to the real test. A maximum loading value of 120kN was applied to specimen I (compressed type)

At the loading rate of 50 kN/min to the central line of the rail head and then removed at the same speed and 100kN for Specimen II (shear type). With the

Determined Ogden model of the third order and The Bergstrom-Boyce model, Quasi-static tests of the two fastening systems were simulated with Abaqus. [5] Stress-based fatigue reliability analysis of the rail fastening spring clip under traffic loads: carried out to develop a method for fatigue reliability analysis of Vossloh spring clip under fatigue random loading. A FEM of the track is programmed dynamically for obtaining the response time history of the Vossloh spring clips displacement under the simulated random traffic loading. Then the results of this analysis as input variable is fed into the FE software to achieve the variable amplitude of stress in critical region. A reliable FEM was constructed for the dynamic stress analysis of SKL14 and the stress concentrated regions as well as the critical dynamic values were recognized in spring clips.

2.2 Stiffness of fastening systems

The stiffness of a fastening system is one of the most important characteristics that Directly impacts the fastening system's long-term performance under repeated axle loading. Stiffness

closely relates to the degree of wear fastening system Components experience and the resulting life of the system. The dynamic rail / Fastening system interaction can be viewed as a complete set of springs and Dampers [6]. The stiffness of each component determines how much the rail is allowed to move within the rail seat [6]. For the purpose of studying fastening system component behavior, it is possible to isolate a force vector and analyze how each fastening system component will perform under a discrete loading event.

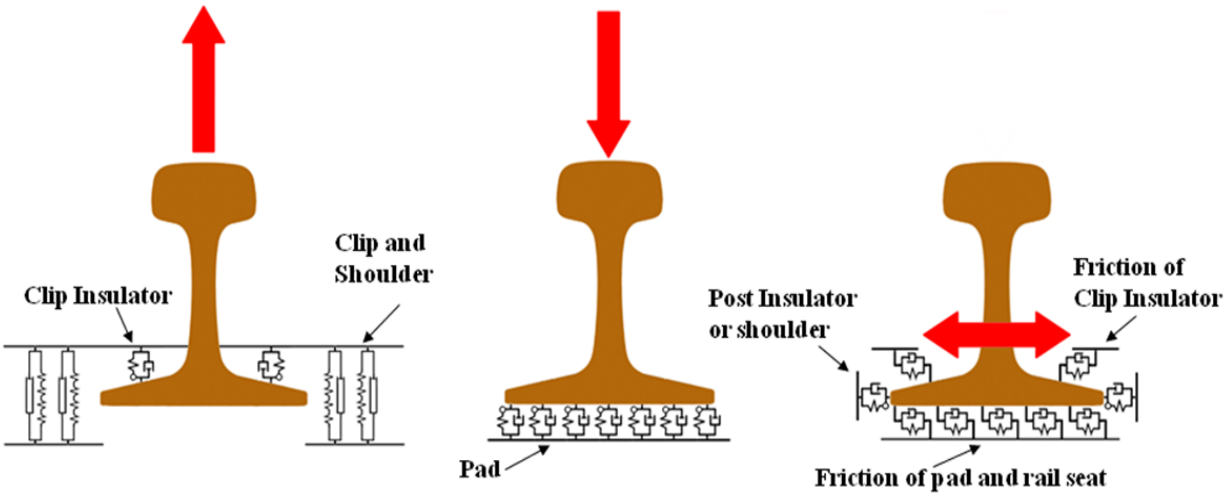

Figure 2.1 the dynamic interaction of the rail, tie, and fastening system

2.3 Types of Fastening Systems

Fasteners are typically classified into two categories: rigid and elastic. Rigid fasteners refer to systems developed in the early 1900s that rigidly bolted the Rail to the tie. Rigid fasteners were superseded by elastic fasteners, which allow more Resilience relative to rigid fasteners. Resilience, which is also referred to as elasticity, is a proxy for the amount of movement the rail experiences within the Rail seat. By design, most of today's fastening systems allow some Resilience to facilitate load attenuation. Within elastic fastening systems, there are large Variations in design resilience and the degree of resilience that is tolerated in the field.

Elastic fastening systems have four primary components; an imbedded anchor, a clip or spring, an insulator, and a pad (or pads) between the rail and concrete tie. Each of these elements is designed to perform a specific function within the fastening system. The clip or spring is

designed to apply an appropriate clamping force (toe load) to the base of the rail. The clamping force is one factor that determines the rigidity of the fastening system. The anchor is designed to hold the clip or spring to the tie, and is cast-in during the tie manufacturing process.

Tie pad is designed to properly attenuate the loads exerted by the rail onto the tie, And should be constructed of a material that is averse to wearing the concrete rail Seat and the base of the rail. The insulator is designed to properly insulate the fastening system from the rail to facilitate reliable operation of the signal system.

In bolted or screwed clip systems, the clip is anchored by a bolt or screw which is threaded into an insert that is cast into the concrete. Bolted or screwed clip systems generally have the advantage of allowing field adjustment of clamping forces. Additionally, many designs allow for efficient replacement of components in the field (clips, bolts, and/or screws). With some bolted clip systems, it is possible to vary rail height in order to maintain proper track geometry. A Disadvantage for some bolted or screwed clip systems is that their installation Tends. To be operator-sensitive, thus it is difficult to achieve a consistent clamping Force at every rail seat without the use of specialized tools or machinery. In some bolted or screwed clip systems, it is important to identify whether the movable portion of the clip is fixed onto the bolt or screw. If it is, the movable portion of the clip tends to loosen the bolt or screw and the fastening system will

Need to be inspected to ensure there is no loss of torque. Driven clip systems generally include a cast-in steel shoulder (or anchor) and a clip, which is driven into the shoulder to achieve the required clamping force. These systems tend to be less operator-sensitive since their correct installation can be confirmed by visual inspection. Captive driven clip systems (which are fully

Assembled with the tie at the tie manufacturing plant) are generally less labor- Intensive to install and remove. One possible disadvantage of driven clip systems is the inability to make adjustments in the field to vary the clamping force. Table 1.1 Compares the clamping force and provides the year of introduction for common Concrete-tie fastening systems used in North American heavy-haul service. [7]

Classification	**Manufacturer**	**Model/ System**	**Nominal Clamping Force per**	**Year of Introduction in North**

			Rail Seat (lbs.)	**America**
Screwed Clip	Vossloh	W with SKL 1	4100	1987
Screwed Clip	Vossloh	W 14 HH with SKL 14R	5400	2006
Screwed Clip	Vossloh	W 30 HH with SKL 30	5400	2009
Driven Clip	Pandrol	PR	4000	1974
		E-Clip	5500	1986
Driven Clip	Pandrol			
		Safelok I	4800	1988
Driven Clip	Pandrol			
		Safelok III	5800	2000
Driven Clip	Pandrol			
		Fast Clip	5500	1992
Driven Clip	Pandrol			
		U 2000 with U2100 shoulder	4800	2001
Driven Clip	Unit Rail			

Table 1.1 concrete tie fastening system used in North American heavy-haul service [7]

CHAPTER THREE

3. MODEL AND FEM ANALYSIS OF RAIL FASTENING SYSTEM USING ANSYS

Concrete tie fastening systems are comprised of various components and materials designed to safely transmit forces exerted by the rail to the concrete tie while restraining the rail to the proper gauge. Forces acting on the fastening system are Vertical, lateral, rotational (both planes), and longitudinal, and are the result of Repeated loading cycles from passing axles, as well as longitudinal stresses in the Rail. Fastening systems components are constructed from a variety of materials (With variable properties) to securely attach the rail to the tie and properly attenuate and/or transfer loads.

3.1 Introduction to Finite Element Method

Finite Element Method is a numerical procedure for solving continuum mechanics of problem with accuracy acceptable to engineers. Finite Element Method is a mathematical modeling tool involving discretization of a continuous domain using Building-block entities called finite elements connected to each other by nodes for once and moment transfer. This process includes Finite Element Modeling and Finite Element Analysis. In displacement based FEM, stiffness of the entire structure (Part or assembly) is assembled from stiffness of individual elements. Loads and boundary conditions are applied at the nodes and the resulting sets of the simultaneous equations are solved using matrix methods and numerical techniques. In short, FEM is a numerical method to solve ordinary differential equations of equilibrium. Starting with simple linear static stress and heat transfer analysis, complex simulations involving highly non-linear, fluid flow and dynamic events can be successfully analyzed on a personal computer using a host of popular software like ANSYS. In practice, a finite element analysis usually consists of three principal steps. Preprocessing: Create and discretize the solution domain into finite elements. This involves dividing the domain into sub-domains, called 'elements', and selecting points, called nodes, on the inter-element boundaries or in the interior of the elements. Assume a function to represent the behavior of the element. This function is approximate and continuous and is called the "shape function". Function". Develop equations for an element. Assemble the

elements to represent the complete problem. Apply boundary conditions, initial conditions, and the loading. Analysis: Solve a set of linear or nonlinear algebraic equations simultaneously to obtain nodal results, such as displacement values, or temperature values, depending on the type of problem.

3.2 Rail

Rails support and guide the wheels of the train vehicles. Rail profile has been the Object of continuous improvement since the beginning of railways. The cross- sections of gauge rails have been standardized by the UIC.

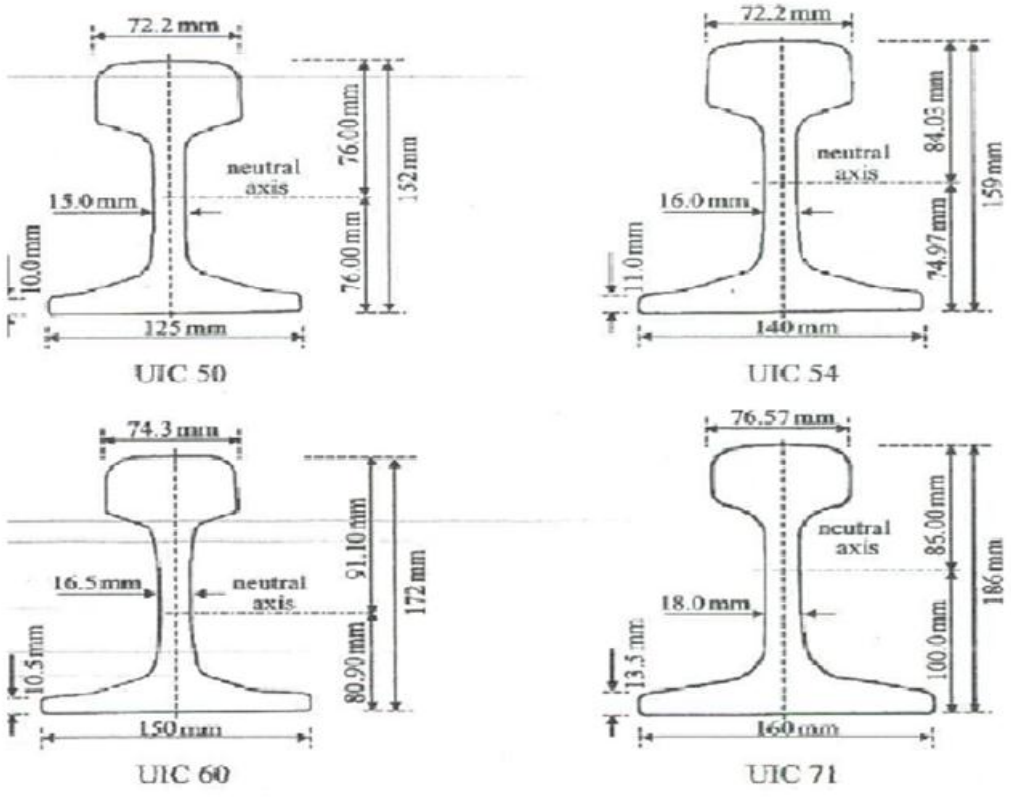

Figure 6: Rail profiles UIC 50 (50 E1), UIC 54 (54 E1), UIC 60 (60 E1) and UIC 71 (71 E1) [11]

UIC50 has been chosen to design and analyze. At first we notice the sizes offered by Vossloh conifer's company, these sizes have been shown in the table below:

Table3.1: The parameters of used rail UIC50.

Parameters.	Dimensions in(mm)
The overall height of the rail	152
The width of rail	125
The height of railhead	49.4
The width of railhead	72.2

The rail is designed as a beam with the cross section of a UIC 50kg/m standard rail which is presented in Figure 6.Because the rail is interacting with wheel and Transfers the sleepers; it remains the rail cross section profile with exact dimensions, in order to keep the accuracy of the results.

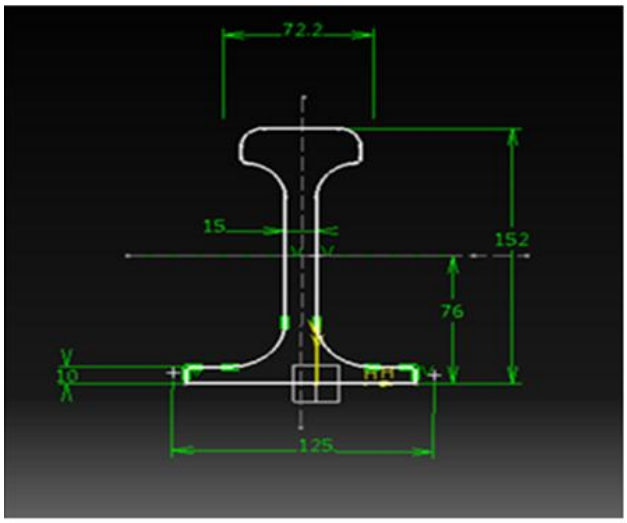

UIC50

Figure3.1: Cross section of 50kg/m standard rail. [11]

Rails are produced in fixed lengths and need to be joined end-to-end to make a continuous surface on which trains may run. However, presence of the fastening absorb the high stress from

the rail, which produces the diverse type of wear or Fracture at the E-clamp fastener .This paper concerns on the stress distribution on Rail fastening under vertical wheel load.

Table 3.2: Dimensions and Specification

Item No	Technical parameters	Values
1	Type of rails for main lines and depot	50kg/m
2	Track gauge:	1435 mm
3	Wheel diameter (new wheel)	≤660 mm
4	Plate length	820 mm
5	Plate thickness	19 mm
6	Sleeper space	625 mm
7	End gap	5 mm
8	Joint bar bolt and nut	M28(AT109)
9	Spring washer	Φ34mm
10	Cross sectional area of rail	64.16cm2
11	Height of the rail	152mm
12	Length of the rail	25m
13	Tram car length	28400mm

Assumptions

- Material properties are isotropic and independent of the temperature;

- The nominal surface of contact between the rail joint and the wheel in Operation is equal to the apparent surface in the sliding motion.
- The contact pressure distributed over friction surfaces is considered as Symmetric.
- The average of the intensity of force into rail E-clamp on the contact area equals.
- The surface of contacting bodies is assumed smooth.
- The wear on the contact surface is negligible.
- The effect of the load is not affected by season.

3.3 E-CLAMP

The E-clamp geometry used by AA-LRT is changed. It is chosen since the Geometry of the AA-LRT E-clamp with curve on new E-clamp but without curve. (See figure below).figure 3.2 shows the different geometry of the two E-CLAMPS: (Figure a with curve and figure b without curve)

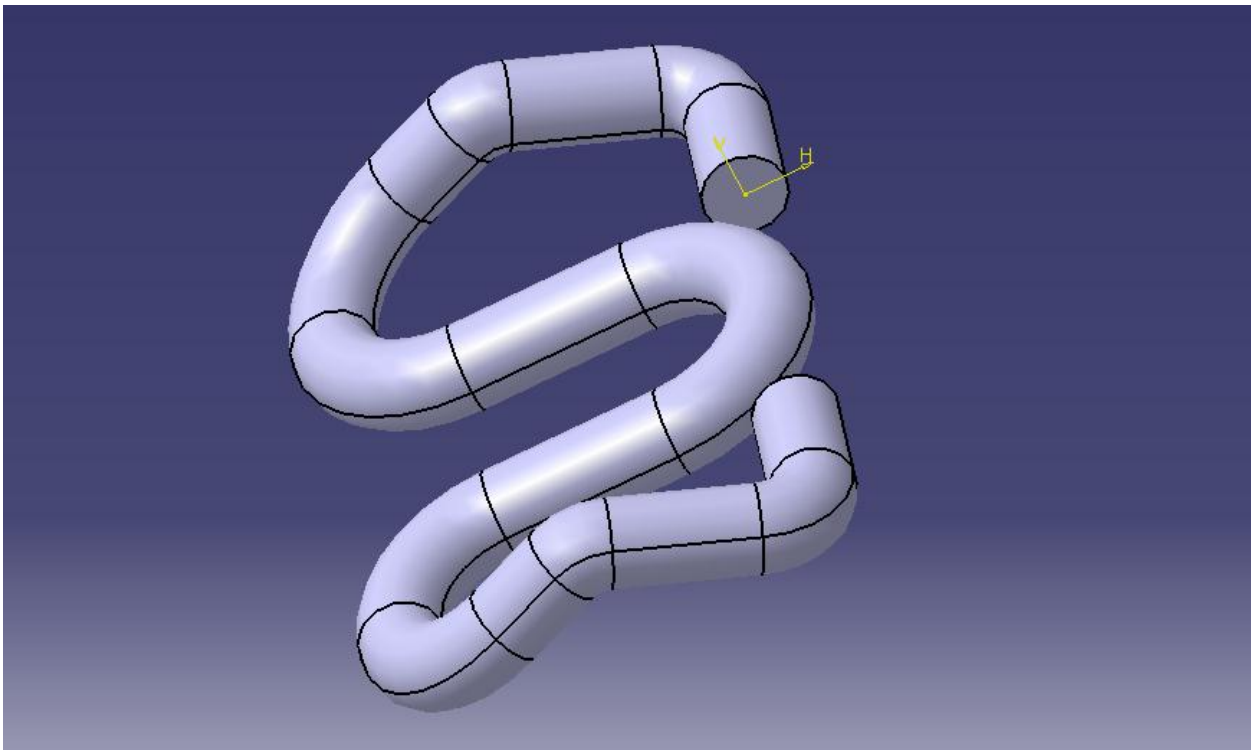

Figure a: E-CLAMP WITH CURVE (from AA-LRT).

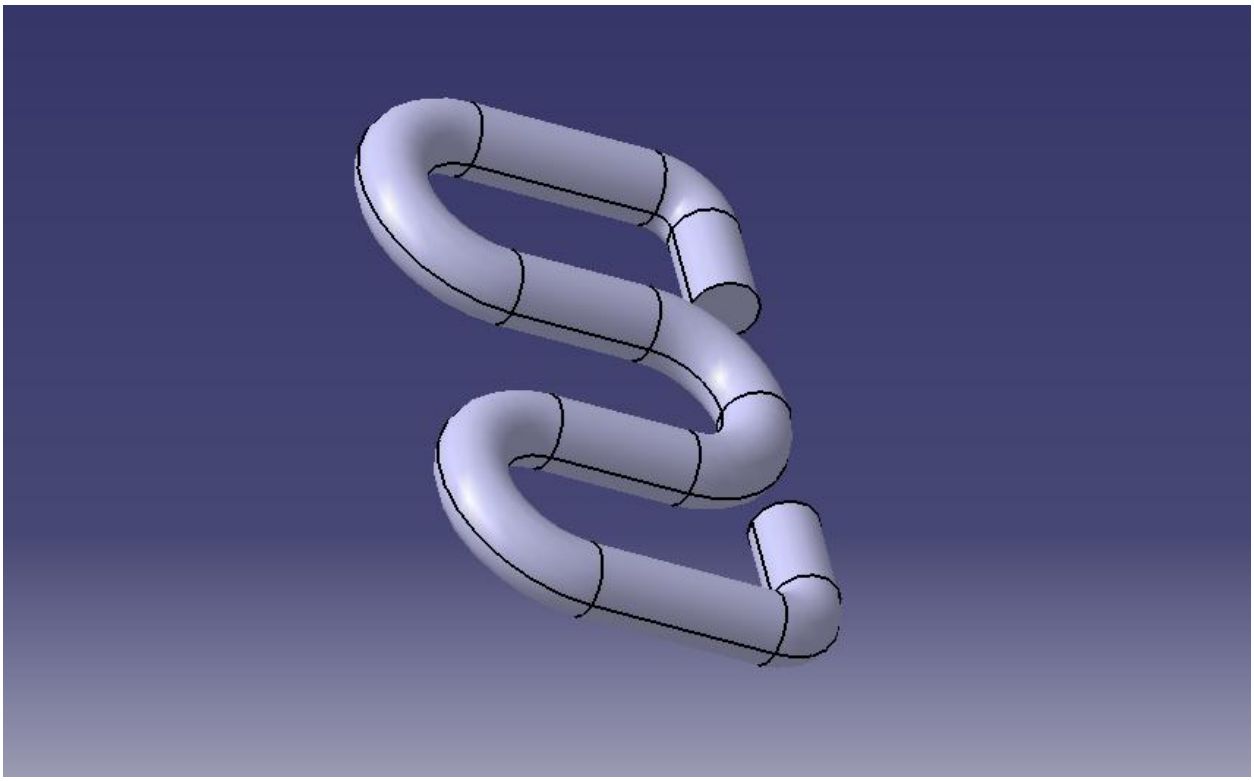

Figure b: E-CLAMP WITHOUT CURVE (new geometry).

3.4 Model and analysis of E-clamp

Fatigue life estimates can be used to guide the selection of inspection intervals for E-clamp in service. A three-dimensional finite element model for rail joint bars is developed and static load is applied to estimate the fatigue life of the joint bars. Different components of the rail fastening are being created separately and assemble in CATIA. The model consists of assembly of the rail, E-clamp, bolts, Nuts, washers, sleeper rail pad and wheel. A three-dimensional finite element Analysis of rail fastening is carried out in ANSYS after importing from CATIA.

Surfaces of engineering components are consistently subjected to contact, thermal and others loading due to these large stresses applied over localized area. Many Researchers studied different parameters and their influence to improve the failurities of the different component of the contact area.

There are different theories, analytical, numerical formula and finite element Method developed in different time to solve the problem related to contact Component and to increase the

performance of the contact area. Although, railway Systems are a transportation system still now it has a large number of unsolved Problems that related to contact surface**.** There are many theories on the contact geometry. However, many published Papers use the hertz theory to understand it easily. The hertz theory has been Developing since [12] Hertzian contact theory, explain a relationship for Determining the contact pressure distribution and contact area of a solid bodies While in contact with an elastic sphere or cylinder under an applied load. This Theory has its own assumption to solve the contact area and stress distribution of two solid bodies.

The following are the hertz theory assumption:-

- The contact between elastic bodies should be frictionless.
- The significant dimensions of the contact area should be much smaller than the dimensions and the radii of curvature of the bodies in contact.
- The contact between elastic bodies should be described by second-order polynomials.

The hertz theory has different type of contact for different shape of the solid body contact. The contact between the wheel/rail is elliptical contact. For wheel/rail contact hertz theory is much preferable than others theory. The analysis of the wheel/rail contact is covered by using the elliptical contact shape to solve the stress, strain, deformation and fatigue life caused by the vertical Load.

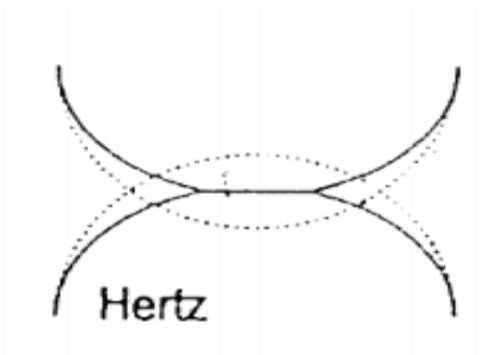

Figure 3.3: Full elastic contact mechanics model of hertz [13]**.**

3.5.1 Modeling Contact at Rail fastening

The wheel profile consists of a flange to guide the trains along the rails and a Conical tread that contacts rail head, and rail has many curvatures to guide wheel properly. The contact positions of the wheel / rail are different in the different Situation. However, this paper uses the contact between the wheels tread and rail head. The contact area between wheel and rail are very small compared to their dimension.

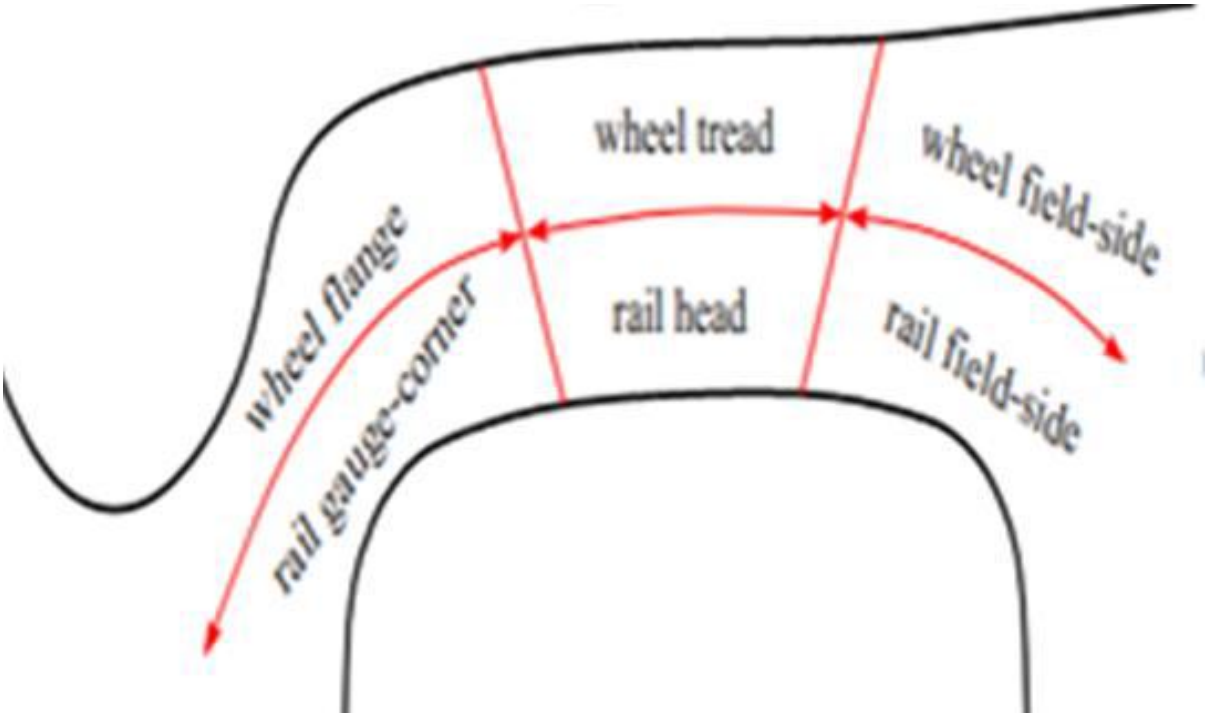

Figure 3.4: Contact zone of wheel/rail

3.5.2 Stress Model Using Hertzian Theory

High stresses are inducing when a vertical load applied on the rail fastening. This can cause serious problem on rail joint. Hertz developed a theory to calculate the Contact area and stress between the two contact surfaces. The purpose of this paper is to focus on the hertz theory, when the wheel and rail contact occur at the end Gap of the rail, however the contact is not a full

contact due to the end gap. As Shown in the figure below the joint bars are connected at rail web, so that the Wheel doesn't contact to the E-clamp.

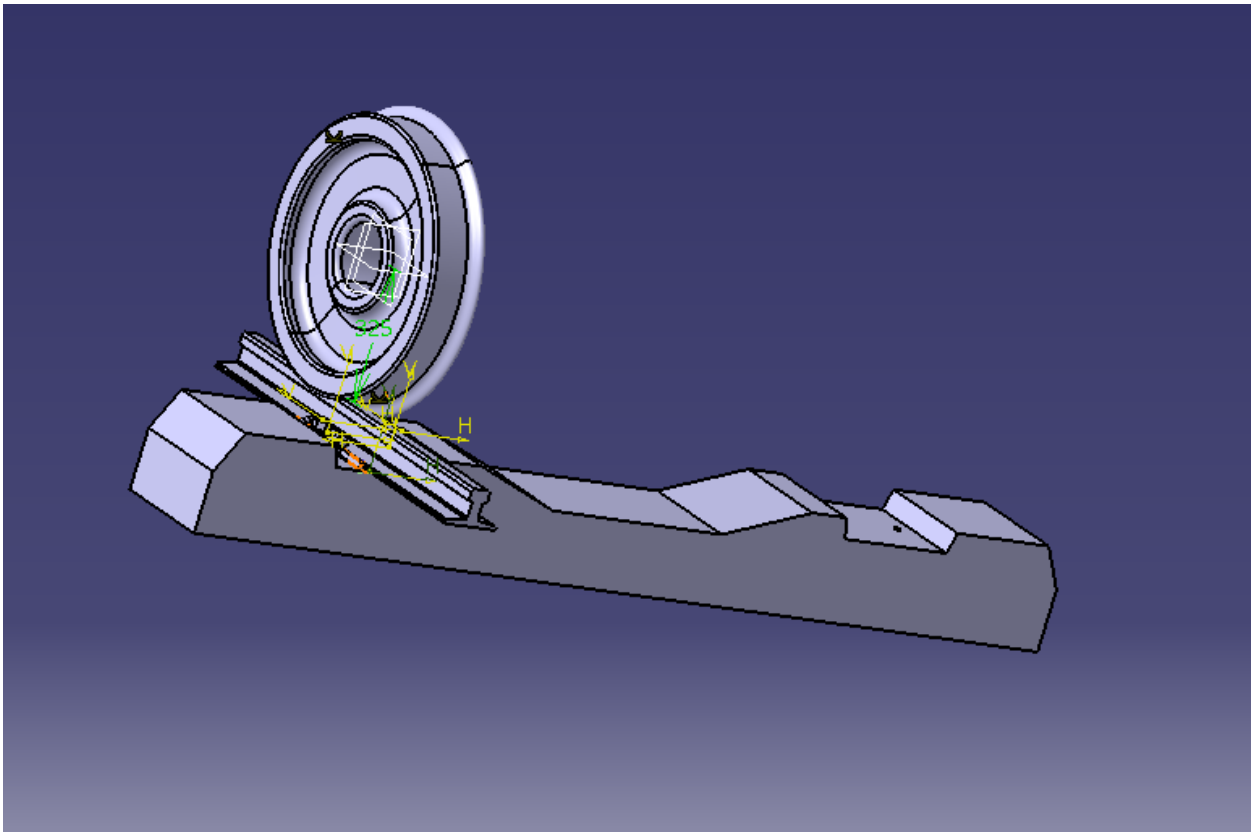

Figure3.5: Wheel/rail contact at rail fastening.

3.5.3 Wheel/rail Contact Mechanics

Surfaces of engineering components are routinely subjected to contact loading, Where large stresses are applied over highly localized area. Many researchers have Studied different parameters and their influence on the dynamic behavior of Rotational system. The stress field created by the contact stresses was first Introduced by [14] Assessment of contact stresses at the wheel–rail interface is one of the most important aspects of railway research, considering the many phenomena involved. For this reason, many scientists have approached the Problem mainly by means of theoretical or numerical solutions based on the Hertz‟s theory, which can be

considered the basic starting point for all subsequent Research. However, there are limiting conditions for the applications of the Hertz
Contact Theory:

i. The contact between elastic bodies should be frictionless,
ii. The significant dimensions of the contact area should be much smaller than the Dimensions and the radii of curvature of the bodies in contact.
iii. The contact between elastic bodies should be described by second-order Polynomials.
iv. An elliptical contact area and an ellipsoidal normal contact pressure distribution are created at contact of the wheel and rail.

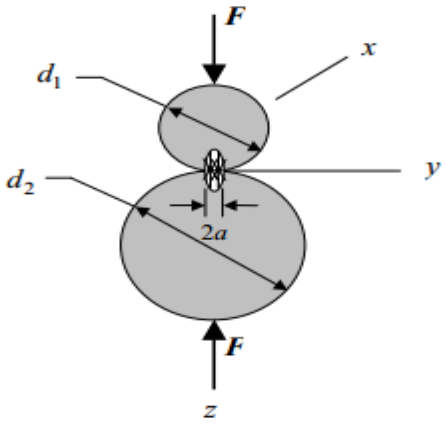

Figure3.6: An elliptical shape of contact stresses [15].

Due the above reason hertz‟s theory applied only for the straight surface and smooth it is not applied on the roughness and fastener part of the rail head. Other method need to analysis the rough surface and fastener part of the rail head. Researcher also used different mechanism to deal the interaction between the wheel and rail. When two elastic non-conforming bodies get together, according to the Hertz contact theory, the contact area is elliptical in shape with a major semi-axis “a” and a minor semi-axis “b”.

The contact pressure distribution in this area represents as semi-ellipsoid, which can beexpressed as:

$$P(r) = p_o\sqrt{1 - \frac{x^2}{a^2} - \frac{y^2}{b^2}} \quad \text{.....3.1}$$

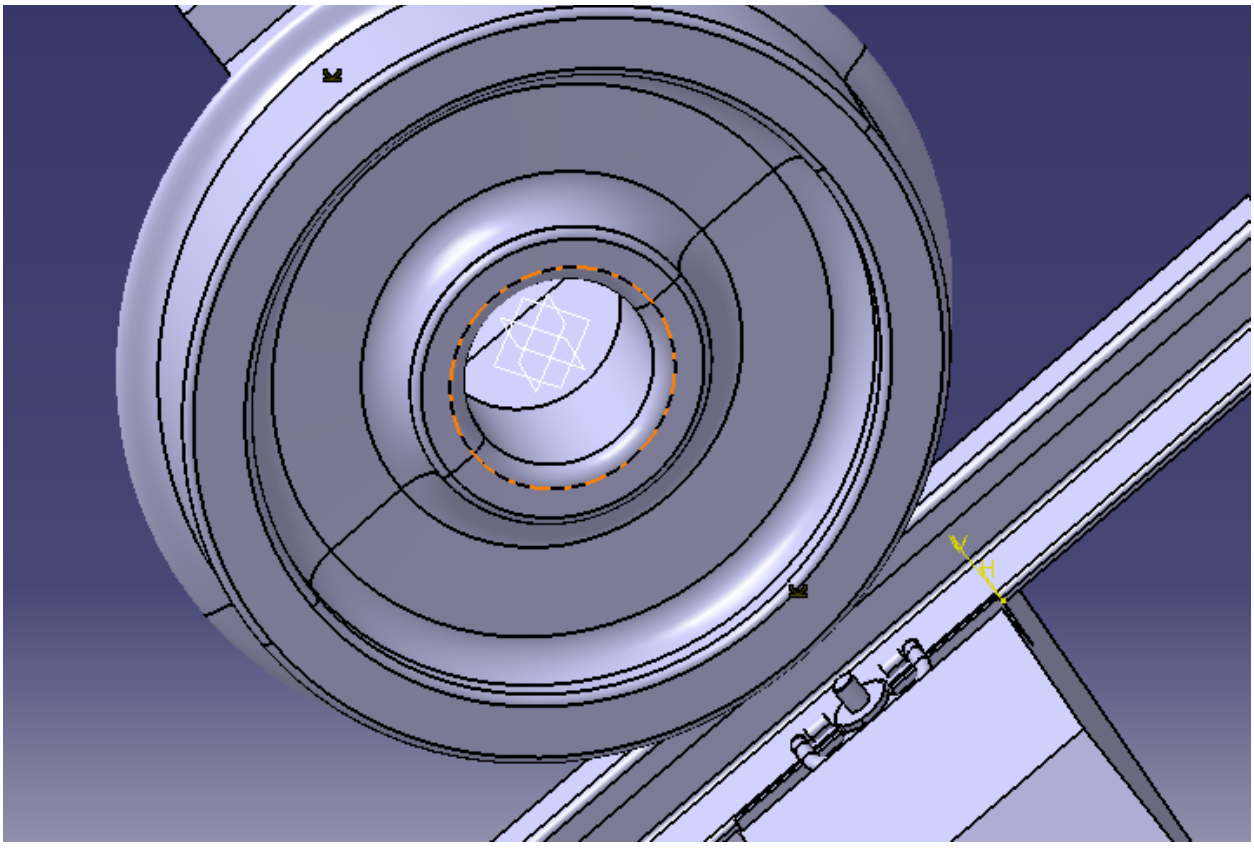

Figure 3.7: Shape of wheel/rail contact

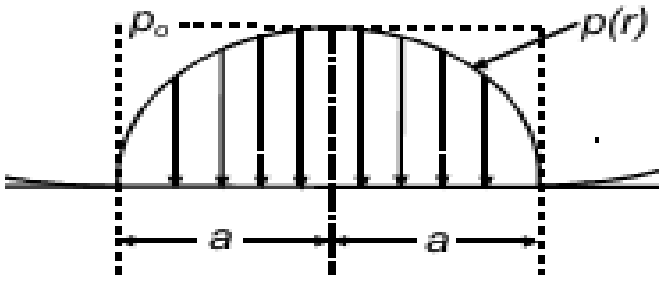

Figure3.8: Pressure distribution at contact zone [16]

Based on the Hertz contact theory, the contact point is very small relative to the overall dimension of wheel and rail surfaces. This very small contact point has elliptical shape. From the above formula a and b are semi axes of the contact ellipse whereas x and y are the required coordinates to specify the point of contacts on the rail head based on the lateral rail surface parameter.

If x=0 and y=0the point of contact is on the centerline of the rail head the stress is maximum, which is equal to:

$$P = p_o \ ,$$

$$\text{Where } p_o = \frac{3F}{2\pi\, ab} \qquad \text{3.2}$$

F is the vertical load act on the rail head

Based on the size and orientation of the contact, the positions of the contact point may be shifted in different directions based on the direction of x or y. However, based on Hertz contact formula and assumptions, the stress due to wheel/rail contact decreases and becomes zero when it goes far away from the centerline of the rail head. Similarly, the wheel/rail contact stress is inversely proportional to the major and minor axis of the contact ellipse[9].

The contact area determined as follows:

$$a = m\left(3\pi F\left(\frac{K_w + K_r}{4K_3}\right)\right)^{1/3} \qquad \text{3. 3}$$

$$b = n\left(3\pi F\left(\frac{K_w + K_r}{4K_3}\right)\right)^{1/3} \qquad \text{3.4}$$

m and n are Hertz coefficients and they are given as a function of the angle (0^o -180^o)

$$\theta = \cos^{-1}\frac{K_4}{K_3} \qquad \text{3.5}$$

θ is rail curvature

M, n are obtained by θ and from the table below:

Table 3.3: m, n quantities [20]

B	M	N
90	1	1
80	1.128	0.893
70	1.284	0.802
60	1.486	0.717
50	1.754	0.641
40	2.136	0.567
30	2.731	0.493
20	2.778	0.408
10	6.612	0.319

K_w and K_r are constants that depend on the material properties of railway wheel and rail respectively.

$$K_w = \frac{1-(\nu_w)^2}{\pi E_w} \quad \text{..... 3.6}$$

ν_w and E_w are Poisson's ratio and young's modulus of the railway wheel material respectively.

K_w is constants that depend on the material properties of railway wheel.

$$K_r = \frac{1-(\nu_r)^2}{\pi E_r} \quad \text{..... 3.7}$$

$\nu_r$and E_r are Poisson's ratio and young's modulus of rail material

K_r is constants that depend on the material properties of rail.

$$K_3 = \frac{1}{2}\left(\frac{1}{R_{1w}} + \frac{1}{R_{2w}} + \frac{1}{R_{1r}} + \frac{1}{R_{2r}}\right), \quad \ldots\ldots\ldots\ldots\ldots\ldots\ldots\ldots\ldots\ldots\ldots\ldots\ldots\ldots.. \ 3.8$$

$$K_4 = \frac{1}{2}\left(\left(\frac{1}{R_{1w}} - \frac{1}{R_{2w}}\right)^2 + \left(\frac{1}{R_{1r}} + \frac{1}{R_{2r}}\right)^2 + 2\left(\frac{1}{R_{1w}} - \frac{1}{R_{2w}}\right)\left(\frac{1}{R_{1r}} - \frac{1}{R_{2r}}\right) cos2\varphi\right)^{1/2} \ldots\ldots.3.9$$

K_3 and K_4 are depends on the geometric propeties of the two bodies.

R_{1w} and R_{1r} are the principal rolling radii of the wheel and rail respectively.

R_{2w} and R_{2r} are the principal transverese radii of curvature of the wheel and radii respectively.

φ is straight segment curvature of the rail.

The direction of the axes of the contact ellipse can be determined based on the radii of curvature and the rolling radii for the two bodies in contact.

If $\frac{1}{R_{1w}} + \frac{1}{R_{2w}} \geq \frac{1}{R_{1r}} + \frac{1}{R_{2r}}$: the transverse semi axis of the contact ellipse (y direction) is greater than or equal to the longitudinal semi-aixs.

If $\frac{1}{R_{1w}} + \frac{1}{R_{2w}} \leq \frac{1}{R_{1r}} + \frac{1}{R_{2r}}$: the transverse semi axis of the contact ellipse (y direction) is less than or equal to the longitudinal semi-axis.

3.6 Finite Element Theory For Contact Body

Finite element theory is used to show that relationship among the contact force, applied force, support and free displacement of wheel /rail contact. During the formulations of finite element the contact between the wheel and rail is assumed:

- Isotropic
- Homogeneous
- Linear elastic body Ω with boundary conditions

The linear elastic bodies have four boundaries condition as shown in the figure below.

- Γ_1 is the boundary with zero displacement,
- Γ_2 is the boundary where measured displacements are given,
- Γ_3 is the boundary with unknown contact forces F_c and unknown contact deformation or displacements,

- Γ_4 is the boundary where applied forces F_a and the other are free surface except those mentioned above. The displacements on boundary $\Gamma_4$are unknown.

Let's recall the general form of static finite element system, which is

$$KU=F \text{ [8]} \quad \text{……..3.10}$$

K, U and F are stiffness matrix of the system, nodal vector displacement, and nodal vector forces. According to the classification of the boundary, it constructs the finite element equation in the following form:

$$\begin{bmatrix} K_{11} & K_{12} & K_{13} & K_{14} \\ K_{21} & K_{22} & K_{23} & K_{24} \\ K_{31} & K_{32} & K_{33} & K_{34} \\ K_{41} & K_{42} & K_{43} & K_{44} \end{bmatrix} \begin{bmatrix} U_1 \\ U_2 \\ U_3 \\ U_4 \end{bmatrix} = \begin{bmatrix} F_1 \\ F_2 \\ F_3 \\ F_4 \end{bmatrix} \quad \text{……..3.11}$$

K_{ij} and $F_1$are sub-stiffness matrix and vector of reaction forces on the boundary Γ_1.

$\overline{F_2}$ is a vector forces on the boundary Γ_2 with measured displacements, usually there is no force on the measured boundary.

F_c and F_a are vector of unknown reaction or contact forces on the boundary Γ_3 and vector of known applied forces on the boundary Γ_4.

$\overline{U}_1$ and U_2 are known displacements on constrained boundary $\Gamma_1$and measured displacement on free boundary Γ_2

U_3 and U_4 are unknown displacements on contact boundary Γ_3 and unknown displacements on boundary Γ4with known applied force Fa, the free surface with no applied force and the internal nodes where net force is zero.

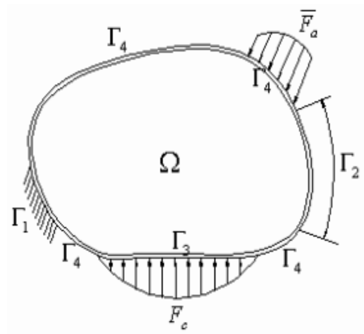

Figure 3.9: Contact model analyze [17].

The stiffness matrix is singular and no unique solution for displacement is possible if the structure is unsupported for the above structure stiffness equation. For this reason all displacement on the boundary $\Gamma_1$are zero, that means U_1=0.When apply this condition to the system matrix and vector in equation 3.11 FEA equation becomes:

Matrix and vector in equation 3.11 FEA equation becomes:

$$\begin{matrix} K_{22} & K_{23} & K_{24} \\ K_{32} & K_{33} & K_{34} \\ K_{42} & K_{43} & K_{44} \end{matrix} \quad \begin{matrix} U_2 \\ U_3 \\ U_4 \end{matrix} \quad \begin{matrix} F_2 \\ = Fc \\ F_a \end{matrix} \quad \text{……} 3.12$$

To calculate the contact forces F_c at U_2. Multiple 3rd row of the stiffness matrix with displacement matrix, then equation became:

$$K_{42}U_2 + K_{43}U_3 + K_{44}U_4 = Fa \text{……} 3.13$$

$$U_4 = K_{44}^{-1}[Fa - K_{42}U_2 - K_{43}U_3] \quad \text{……} 3.14$$

Multiple the 2nd a row with displacement column, the equation became;

$$K_{32}\,U_2 + K_{33}U_3 + K_{34}U_4 = F_c \quad \text{3.15}$$

$$U_3 = K_{33}^{-1}\,[Fc - K_{32}U_2 - K_{34}U_4] \quad \text{3.16}$$

When equation 3.13 substitute in the equation 3.14, U3 became;

$$U_3 = K_{33}^{-1}[F_c - (K_{33} - K_{34}\,K_{44}^{-1}\,K_{43})\,U_2 - K_{34}K_{44}^{-1}F_a + K_{34}K_{44}^{-1}K_{43}\,U_3] \quad \text{3.17}$$

Therefore the displacement at the contact point is:

$$U_3 = K_{33}^{-1}[F_c - (K_{33} - K_{34}\,K_{44}^{-1}\,K_{43})\,U_2 - K_{34}K_{44}^{-1}F_a + K_{34}K_{44}^{-1}K_{43}\,U_3] \quad \text{3.18}$$

Generally, the contact between the wheel and rail are considered to determining the failure effect of rail end and rail joint. Stress -strain relationship of structural analysis

$$\{\,\boldsymbol{\sigma}\,\} = \{K\}\,\{\,\epsilon^{el}\} \quad \text{3.19}$$

ϵ^{el}, σ and D are elastic strain vector, stress vector and elastic stiffness matrix.

$$\{\,\boldsymbol{\sigma}\,\} = \{\,\boldsymbol{\sigma}x, \boldsymbol{\sigma}y, \boldsymbol{\sigma}z, \boldsymbol{\sigma}xy, \boldsymbol{\sigma}yz \text{ and } \boldsymbol{\sigma}xz\} \quad \text{3.20}$$

$$\{\,\epsilon^{el}\} = \{\epsilon\} - \{\epsilon\}^{th} \quad \text{3.21}$$

$$\{\epsilon\} = \{\epsilon\}^{th} + \{D^{-1}\}\{\boldsymbol{\sigma}\,\} \quad \text{3.22}$$

$$\{D^{-1}\} = \begin{bmatrix} 1/E_x & -\nu_{xy}/E_x & -\nu_{xy}/E_x & 0 & 0 & 0 \\ -\nu_{yx}/E_y & 1/E_y & -\nu_{yz}/E_y & 0 & 0 & 0 \\ -\nu_{zx}/E_z & -\nu_{zy}/E_z & 1/E_z & 0 & 0 & 0 \\ 0 & 0 & 1/G_{xy} & 0 & 0 & 0 \\ 0 & 0 & 0 & 1/G_{yz} & 0 & 0 \\ 0 & 0 & 0 & 0 & 0 & 1/G_{xz} \end{bmatrix} \quad \text{3.23}$$

E_x and G_{xy} are young's modulus in the x direction and shear modulus in the xy plane

V_{xy} and v_{yx} are major poison's ratio and minor poison's

Also the $\{D^{-1}\}$ matrix is presumed to be symmetric, so that

$$\frac{v_{xy}}{E_y}=\frac{v_{xy}}{E_x} \quad \text{.....3.24}$$

$$\frac{v_{zx}}{E_z}=\frac{v_{xz}}{E_x} \quad \text{.....3.25}$$

$$\frac{v_{zy}}{E_z}=\frac{v_{yz}}{E_x} \quad \text{.....3.26}$$

$$\frac{v_{zx}}{E_z}=\frac{v_{xz}}{E_x} \quad \text{.....3.27}$$

$$\frac{v_{zy}}{E_z}=\frac{v_{yz}}{E_y} \quad \text{..... 3.28}$$

The element integration point strain and stress are:

$\{\in^{el}\}= \{B\}\{U\} - \{\in\}^{th}$, for this case, $\{\in\}^{th}$ is zero 3.29

$\{\boldsymbol{\sigma}\} = \{D\}\{\in^{el}\}$ 3.30

B and$\{\in\}^{th}$ are strain - displacement matrix evaluated at integration point and thermal strain

$\in^{el}$ is strain that cause stress

Maximum stress failure criteria

$$\boldsymbol{\varepsilon_x} = \text{maximum of} \left\{ \frac{\sigma_{yc}}{\sigma_{yc}^f}, \frac{\sigma_{xy}}{\sigma_{xy}^f}, \frac{\sigma_{yz}}{\sigma_{yz}^f}, \frac{\sigma_{zc}}{\sigma_{zc}^f}, \frac{\sigma_{zx}}{f_{\sigma zx}} \right\} \quad \text{..... 3.31}$$

σ_x, σ_y and σ_z are stress in x, y, z direction

σ_{xc}^{f} , σ_{yc}^{f} $andz$ are normal stress failure in x, y, z direction.

σ_{xy},σ_{xy} andσ_{xy} are shear failure in xy, yz, xz direction.

3.7 Geometrical Model

In the three-dimensional model of rail joint and wheel, single surface of its symmetry in axial direction is not insulated owing nature of considered phenomenon of loading. It has six holes to fasten bolts. The geometry of the rail on CATIA is illustrated in Fig 3.10.

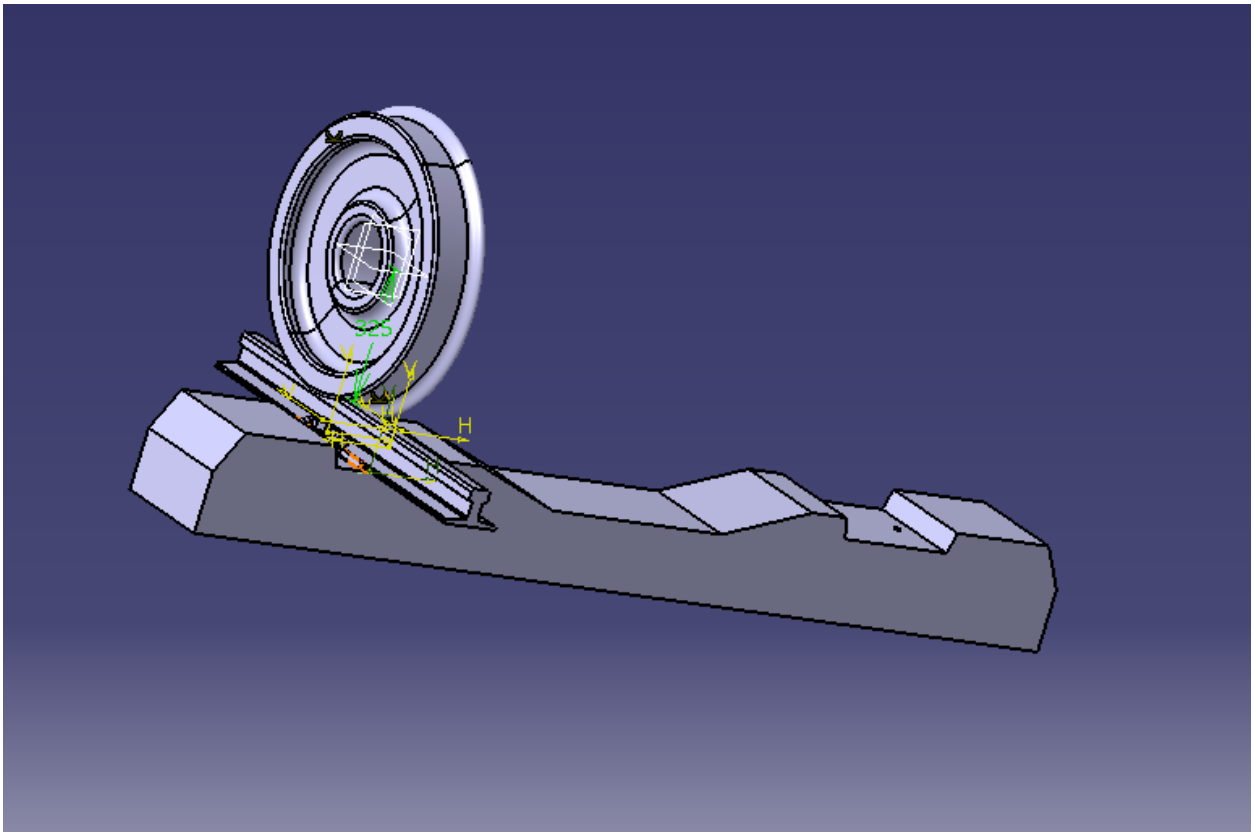

Figure 3.10: 3D model of wheel /rail contact at a rail fastening

3.8. Definition of Material

Materials of the rail fastening given the principal requirements involved, the steels generally used for wheels and rails have a predominantly pearlitic microstructure incorporating hard

cementite lamellae that guarantees high resistance to wear. The microstructure produced by transformation close to thermodynamic equilibrium simultaneously ensures more sluggish transformation in operation than, for instance, a bainiticor martensitic microstructure [18]

3.8.1Material selection

The railway tracks are mostly steel material in accordance to the EN 13674-1:2011 (E). It can be produced with tensile strengths exceeding 5 GPa. Steel contains 50% iron and one or more alloying element.

These elements generally include carbon, manganese, silicon, chromium, phosphorus, sulpher etc. Each element has a specific role in the steel making process or in achieving particular properties E.g. Strength, hardness and quality. Most of the materials used in this specific project are based on Addis Ababa Light rail Transit (LRT). In this study the wheel has approximately similar material properties to the rail. Properties of joint bars and rail are the same for the simplicity of the problem, but for the concrete sleepers with a density of 2300kg/m3.

Table 3.4: Mechanical property of rail material

Item No	Mechanical property	Value
1	Poison'sRatio	0.3
2	Young's Modulus (MPa)	207 MPa
3	Ultimate tensile strength (MPa)	880 MPa
4	Yield strength	640 MPa
5	Density	7800 kg/m
6	Elongation	12 %

Table 3.5: Mechanical property of *Concrete* material

	Young's modulus, MPa	*Poisson's ratio*	*Density, kg/m3*
Concrete	*300000*	*0.18*	*2300*

Table 3.6: Chemical composition of rail

Item No	1	2	3	4	5	6
Chemical element	C	Si	Cr	Mn	P	s
Composition	0.8	08	---	1	0.04	0.05

Table3.7: Mechanical property of joint washer, bolt and nut

Item No	Mechanical property	Value
1	Poison'sRatio	0.3
2	Young's Modulus (MPa)	207 MPa
3	Ultimate tensile strength (MPa)	880 MPa
4	Yield strength	640 MPa
5	Density	7800 kg/m
6	Elongation	12

3.9 Load and Support

Material properties and data are used based on Ethiopia Railway Corporation, Addis Ababa Light rail Transit (LRT). Vertically downward load is sum of 3% allowance, maximum axle load. The overall load is the sum of the total tram weight and carrying capacity of the vehicle. The overall load is classified to each axle of the vehicle then the axle load is classified to each wheel vehicle. Carrying capacity of vehicle has calculated by take average of 60kg/ person and the total rate of passenger inside of the tramcar is 317.

Table 3.8: Seating capacity of vehicle

Item No	Number of passengers (persons)	Seated	Standing	Total
1	Seats (AW_1)	60	5	65
2	Seating capacity (AW_2) (standing: 6 persons/m^2)	65	190	254
3	Overload capacity (AW_3)(standing: 8 persons/m^2)	65	252	317

Table 3.9: Vehicle weight

Item No	Loads	Carbody weight	Passenger weight	Total weight
1	Empty vehicle (t)	44	0	44
2	Seating capacity (t)	44	15.24	59.24
3	Overload capacity (t)	44	19.02	63.02
4	Axle load	≤11（1+3%）t		
5	Axle number	6		

Note: Take 60kg as average weight of each passenger.

3.10 Analysis of Straight Rail fastening Using ANSYS 14.5

3.10.1 Meshing

In the finite element analysis the basic concept is to analyze the structure, which is an assemblage of discrete pieces called elements, which are connected, together at a finite number of points called nodes. A network of these elements is known as a mesh. For this analysis, the model of rail joint was meshed with the tetrahedral finite element were used in ANSYS rather than defining the nodes individually (fig.3.10). The finite elements used for the meshing were Free triangular. The size of the meshing type is medium size mesh.

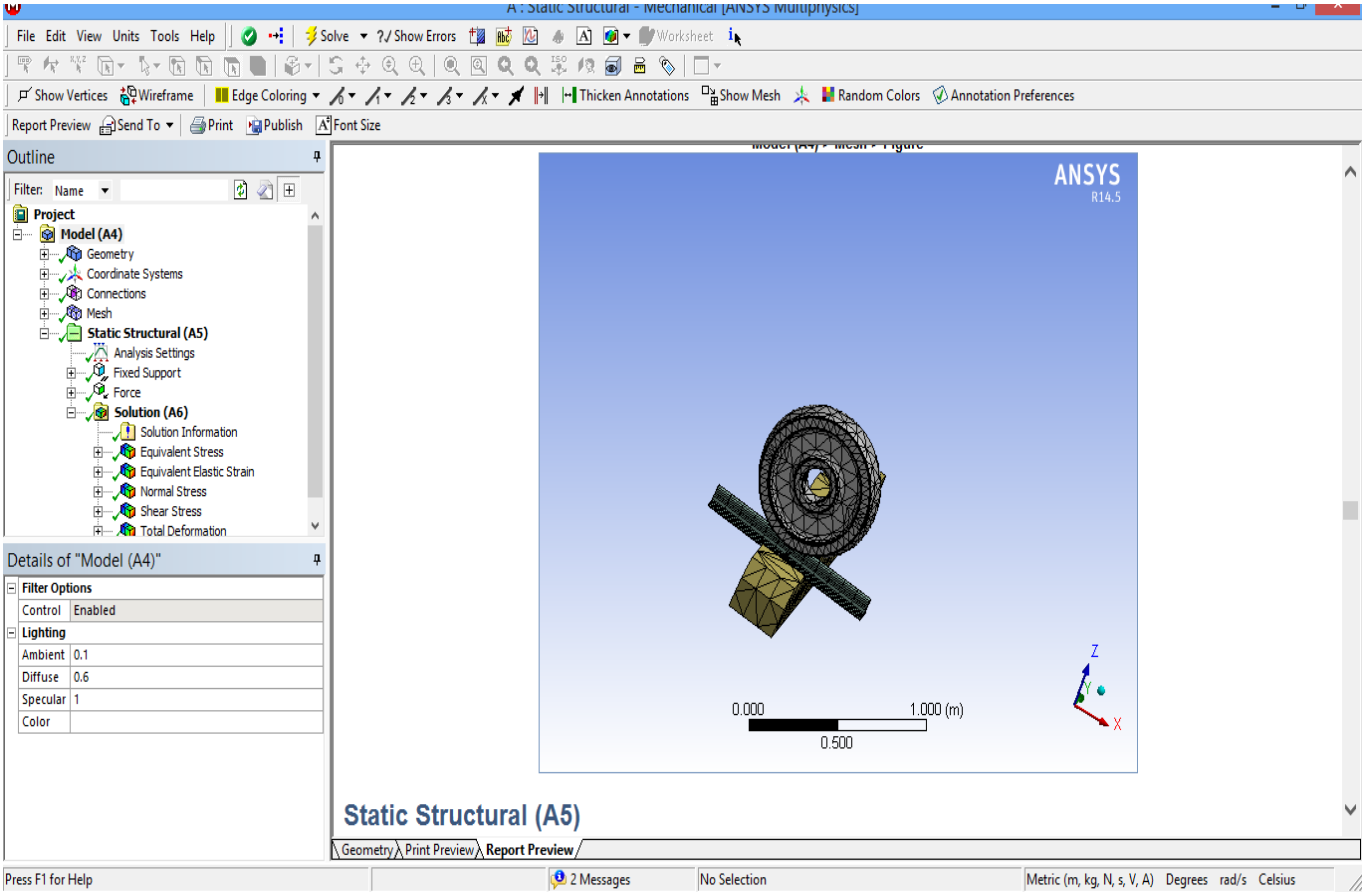

Figure 3.11: Meshed Model of rail fastening

3.10.2 Finite element simulation computation model

A 3-D finite element model for element model for wheel/rail rolling contact is Developed on the most critical section of rail track i.e., rail fastening to calculate Finite element analysis and stress response in the contact region.

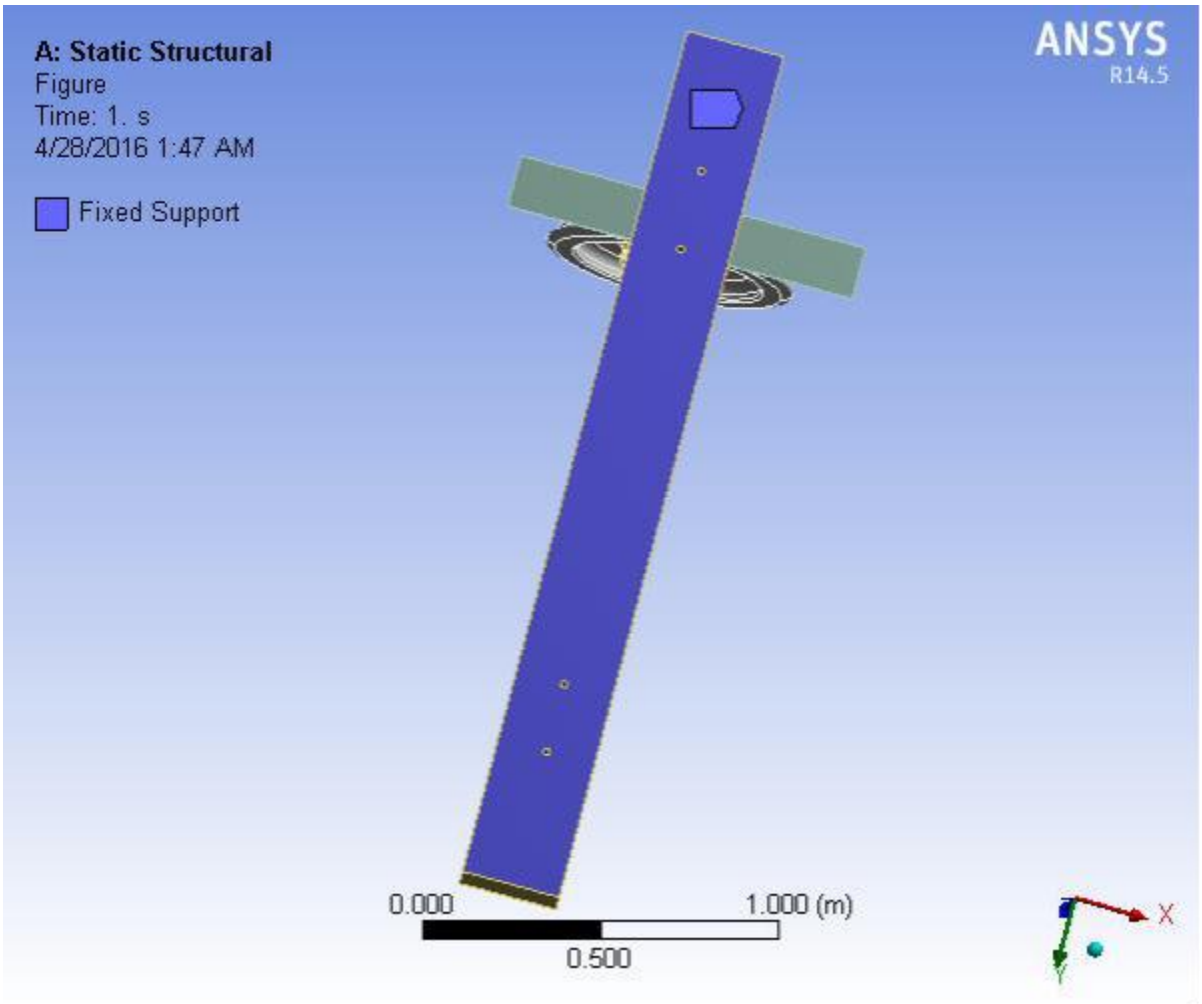

Figure3.14: Finite element modeling of wheel/rail sleeper set

3.10.3 Wheel load

In this model, the load is the static load on wheel, which is applied on the center of wheel. The position of applied load and direction on wheel are shown below. But in case of the tram car we

do have three bogies each having two axles and the wheel load will be one half of the weight of the axle load. The total numbers of the axles are six.

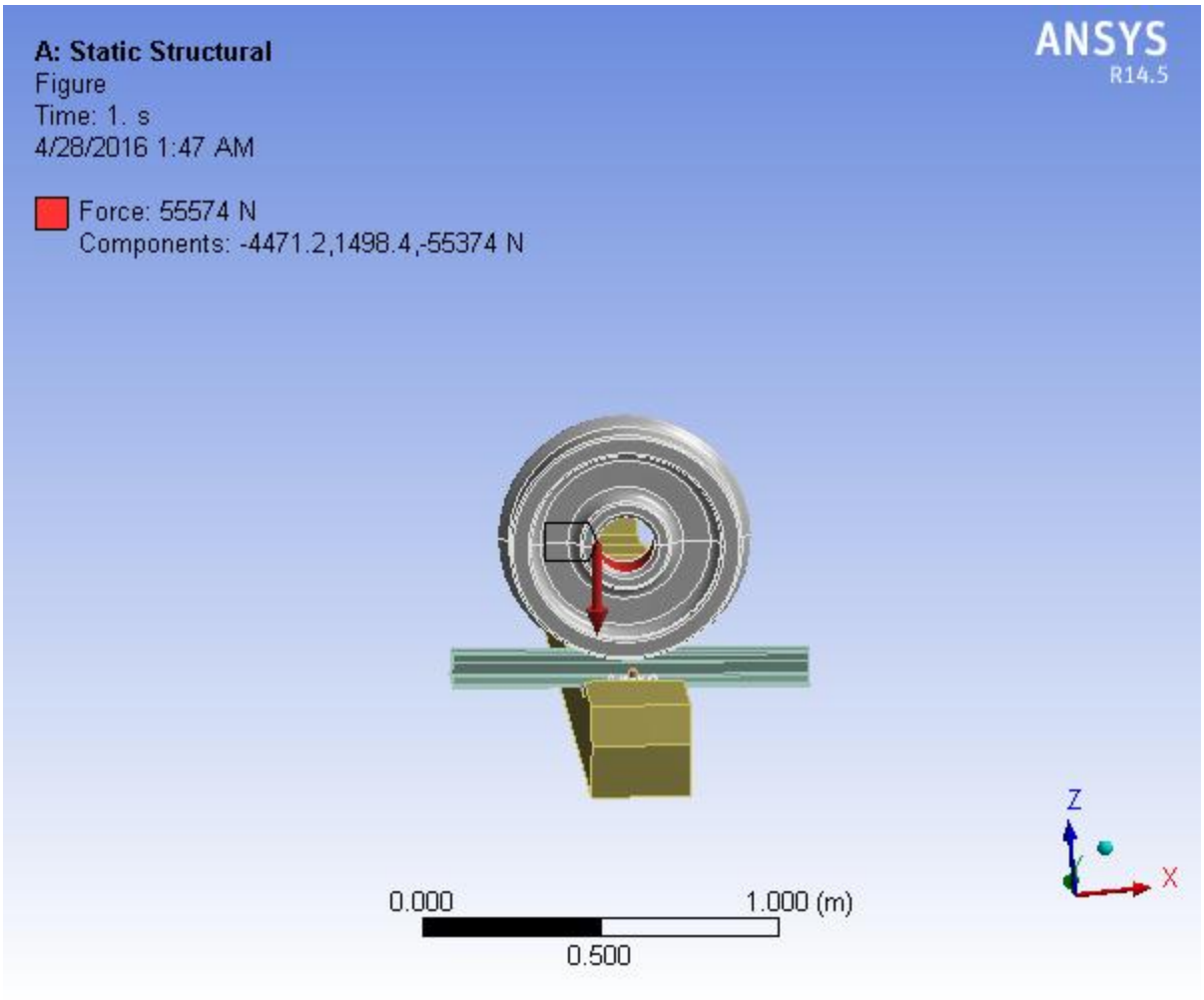

Figure 3.15: the position of applied wheel load

The total vertical load is calculated as follows:

a. Tram car weight = 44 ton
   - The load apply on each axle = 7.333 ton = 73333N
   - The load apply on each wheel = 3.667 ton =36667 N

b. Carrying Capacity = 60kg/person *317 person =19020N

c. Over all capacity = Tram car weight on each wheel + Carrying Capacity

d. Maximum Axle load = 11,000 kg $\times$ 9.81m/s

=107,910N

e. The total vertical load = maximum Axle load +3% maximum Axle load

= 111147.3N

f. The load on each wheel = 55573.63N

3.10.4 Velocity on wheel

As the wheel is rolling on the top of rail0, its velocity has two components, namely the moving velocity and angular velocity. Their relationship is that, the product of angular velocity magnitude and radius of the wheel equals to the magnitude of moving velocity. Table 12.

Table 3.10: Operating speed of tram

Item No	Parameter	Speed
1	Maximum operation speed	70 km/h
2.	Average travelling speed	≥20km/h
3	Operation speed during car wash	3~4 km/h

The maximum operation speed of the tramcar is 70km/h and Wheel diameteris 660mm then the rotational velocity can be calculated as:

From V=wr, $w = \frac{v}{r}$ =70km/h /330mm =58.9225rad/s

The types of loading that can be applied in a static analysis include:

- Vertical wheel load (force).
- Standard earth gravity
- Rotational velocity

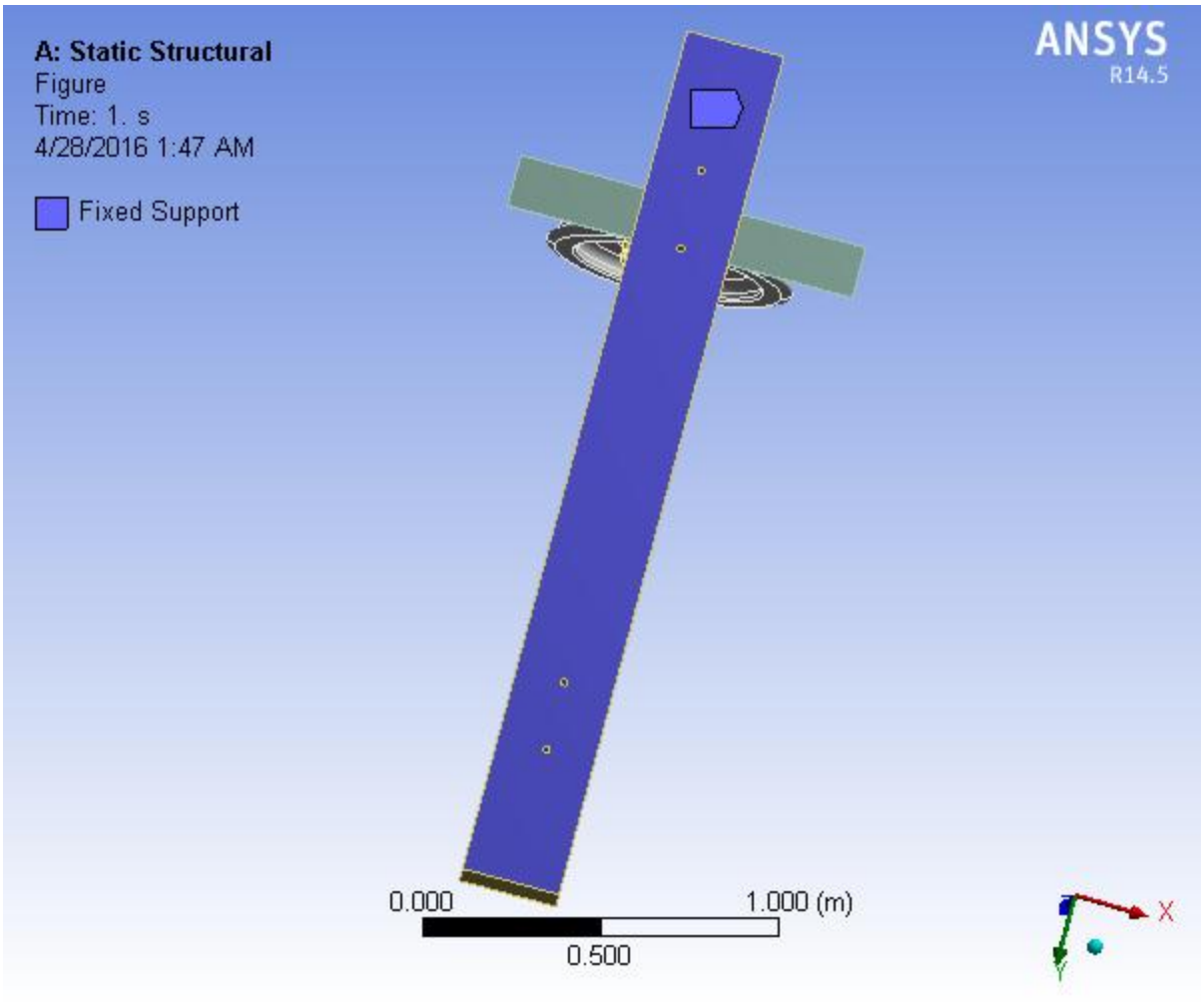

Figure3.17: Fixed support

CHAPTER FOUR

4. RESULT AND DISCUSSION

4.1 Results

The analysis is performed by using finite element model consist of fatigue analysis, to determine the impact of the wheel load on a bolted rail joint. Different support location is used to perform finite element analyses, although the geometry and load application are the same for all support location.

4.1.1. Static Analysis

A static structural analysis is determine the deflection, stresses, strains, safety factor, and fatigue stress of structures caused by loads that do not induces significant inertia and damping effects. The load and the structure responses are assumed to vary slowly with respect to time that means steady loading and response condition are assumed.

4.1.1.1. Stress

Stress is defined as the average force per unit area that some particle of a body exerts on an adjacent particle, across an imaginary surface that separates them.

Case 1: E-Clamp with curve (from AALRT)

A. Equivalent stress (von –mises stress) (Pa)

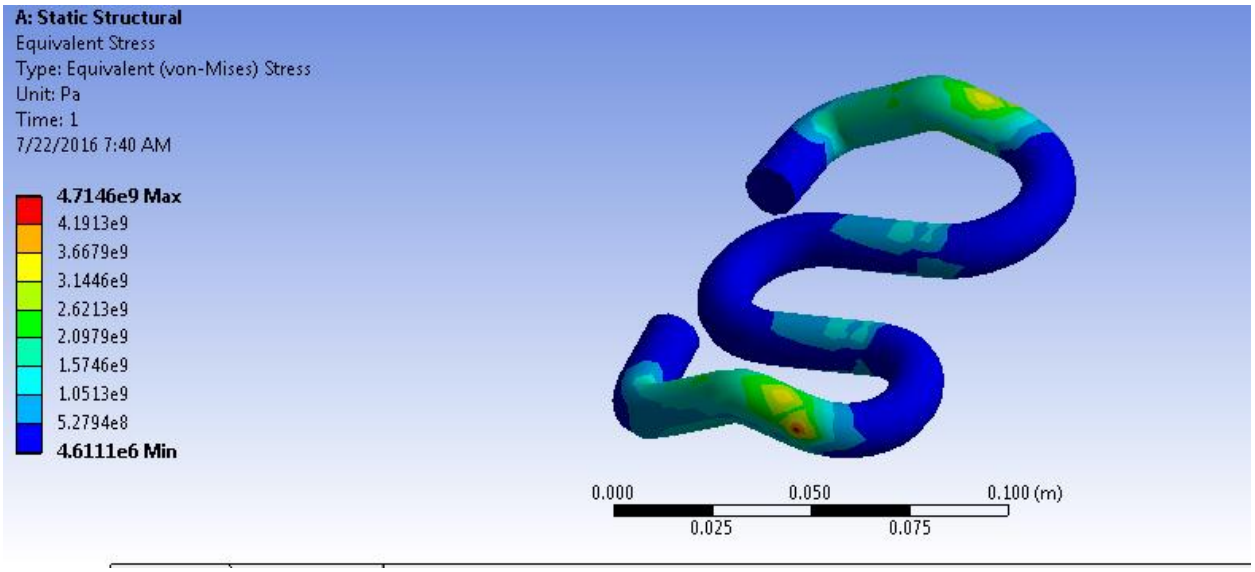

Figure 4.1 Von mises stress of AA-LRT e-clamp

As shown in above figure, the maximum von mises stress is 4714.6MPa and the minimum von mises stress is 4.6111MPa.

B. Normal stress (bending stress) (Pa)

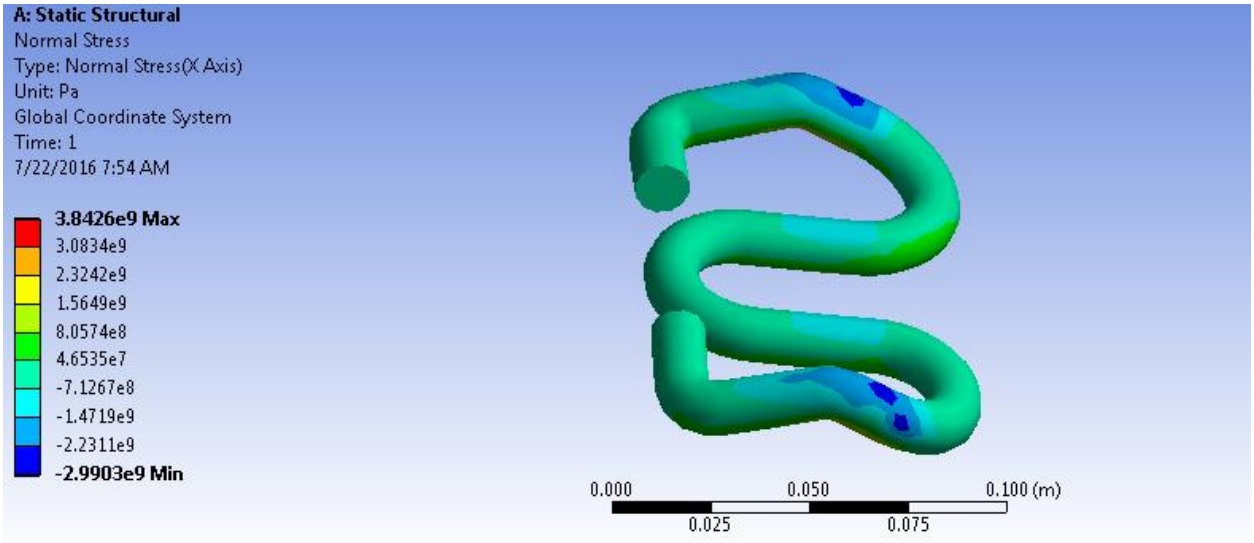

Figure 4.2 Normal stress

As shown in above figure, the maximum normal stress is 3842.6MPa and the minimum normal stress is -2990.3MPa.

C. Shear stress (Pa)

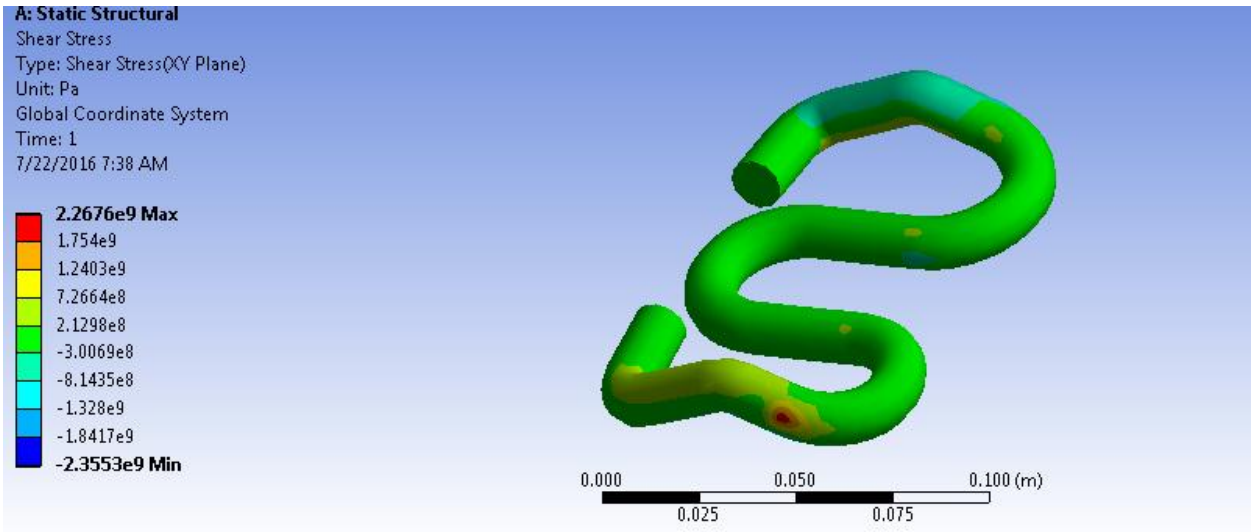

Figure 4.3 Shear stress

As shown in above figure, the maximum shear stress is 2267.6MPa and the minimum shear stress is -2355.3MPa.

Case 2: new geometry E-Clamp without curve

A-Equivalent von mises stress

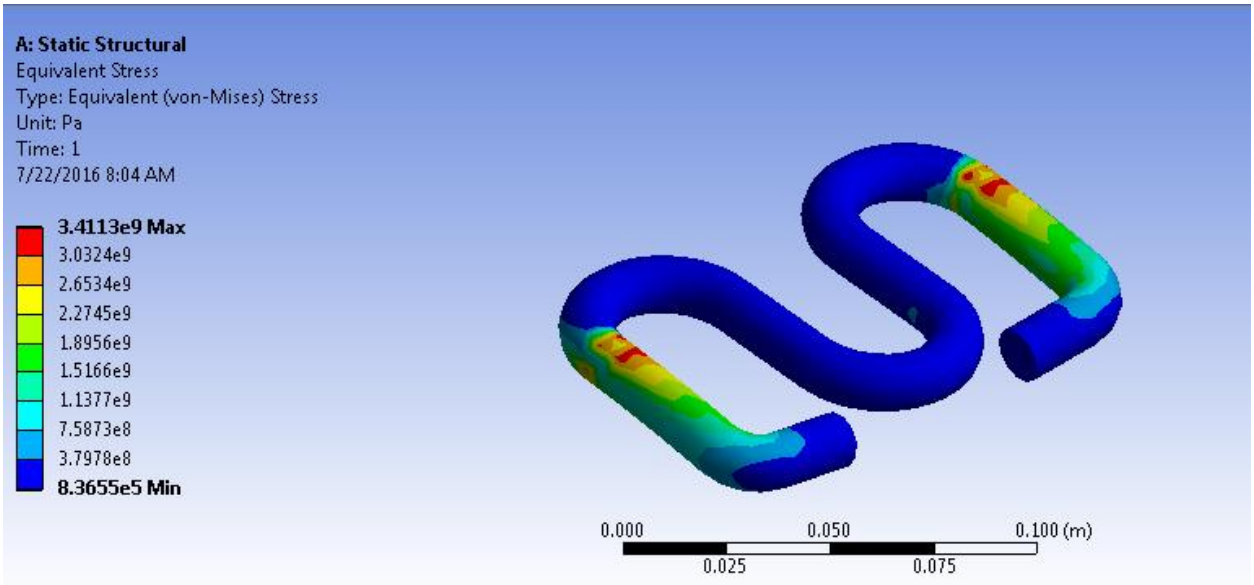

Figure 4.4 Von mises stress

As shown in above figure, the maximum von mises stress is 3411.3MPa and the minimum von mises stress is 0.836MPa.

B. Normal stress (bending stress) (pa)

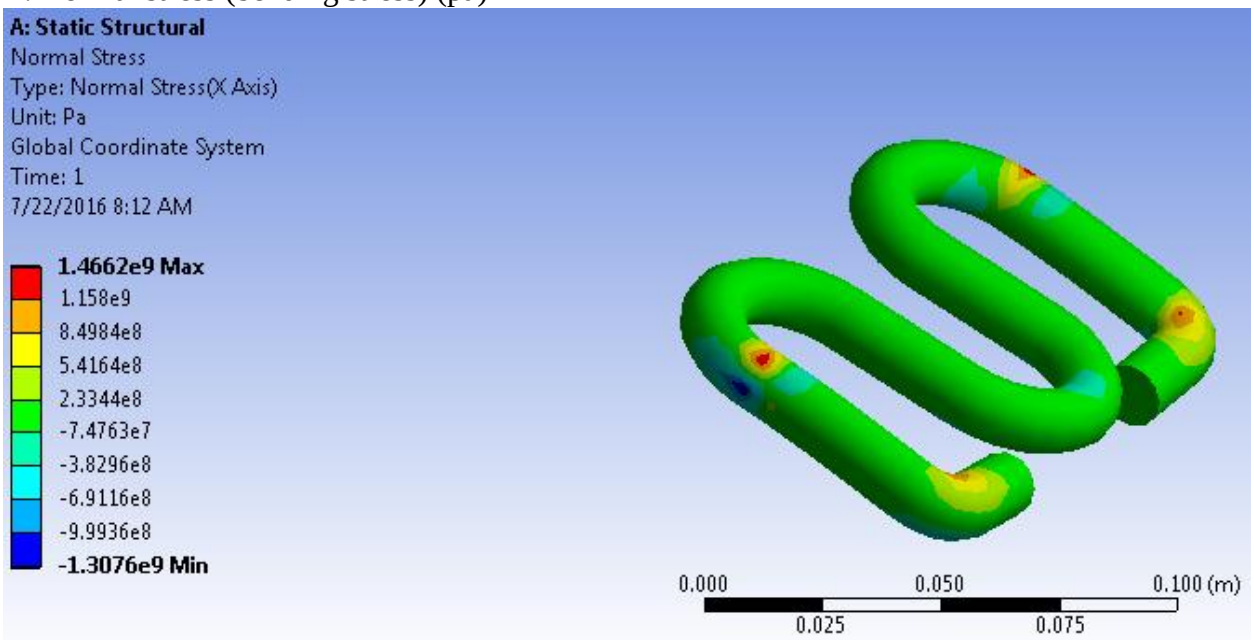

Figure 4.5 Normal stress of new E-clamp

As shown in above figure, the maximum normal stress is 1466.2MPa and the minimum normal stress is -1307.6MPa.

C. Shear stress

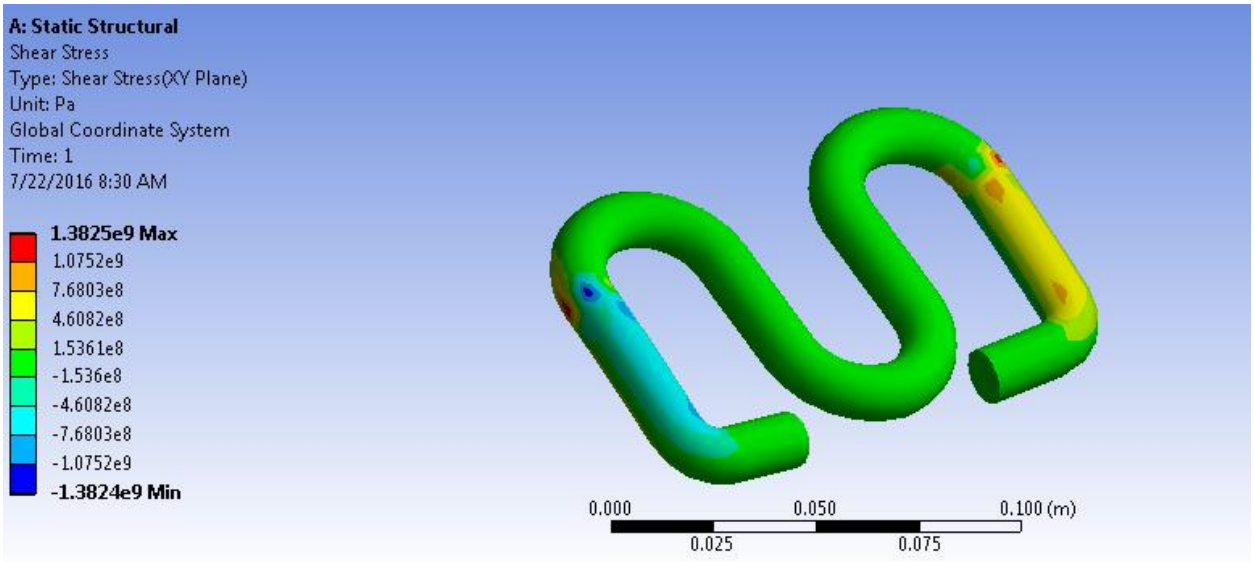

Figure 4.6. Shear stress

As shown in above figure, the maximum shear stress is 1382.5MPa and the minimum shear stress is -1382.4MPa.

The table below shows the comparing the different stress values of research result values of existing E-clamp and new geometry E-clamp using same tram car wheel load.

Table 4.1: von miss stress shear stress and normal stress values of the existing E-clamp and the new geometry E-clamp.

Von mises stress(MPa)	Max Min	4714.6 4.611	3411.3 0.836
Shear stress(MPa)	Max Min	2267.6 -2355.3	1382.5 -1382.4
Normal stress(MPa)	Max Min	3842.6 -2990.3	1466.2 -1307.6

II- **Fatigue analysis**

Case1: existing E-clamp

A-Alternating stress

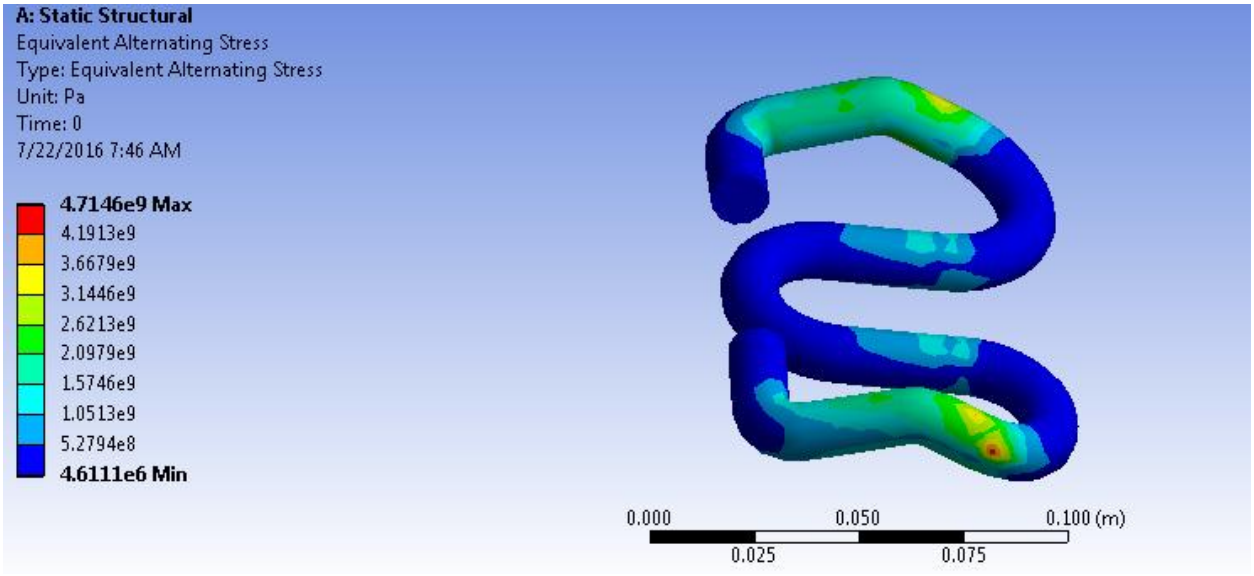

Figure 4.7: alternating stress

As shown in above figure, the maximum alternating stress is 4714.6MPa and the minimum alternating stress is 4.611MPa.

B- Biaxiality indication

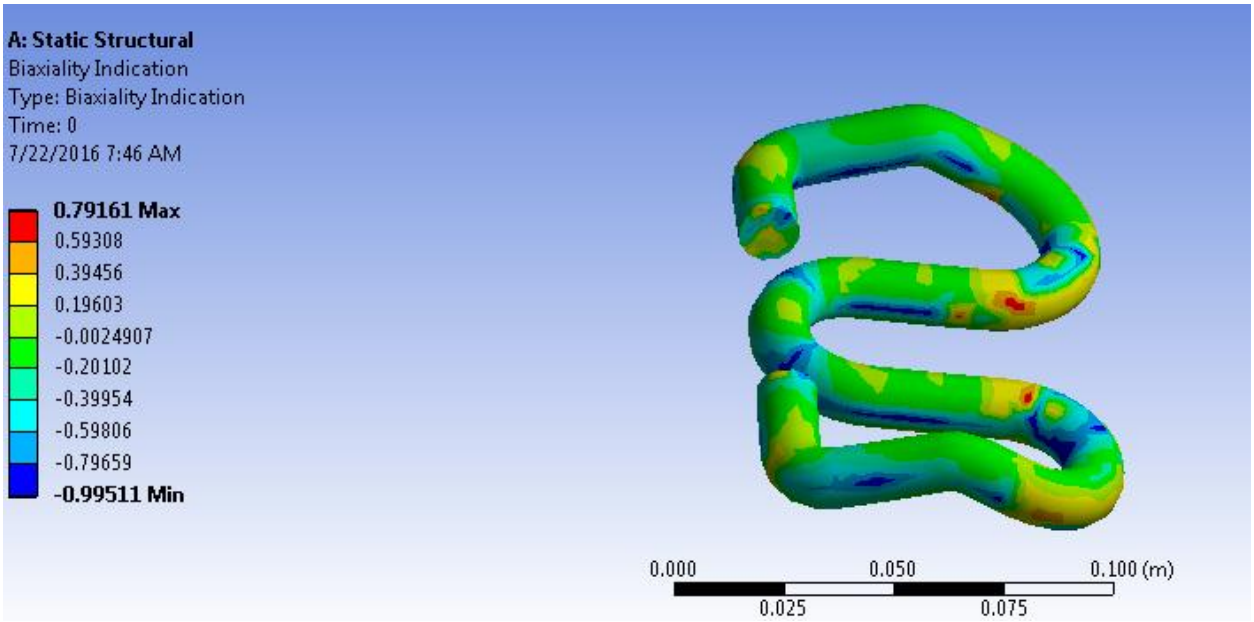

Figure 4.8: Biaxiality indication

As shown in above figure, the maximum biaxial indication is 0.7916 and the minimum biaxial induction is -0.995.

C- Factor of safety/ fatigue life , damage and total deformation

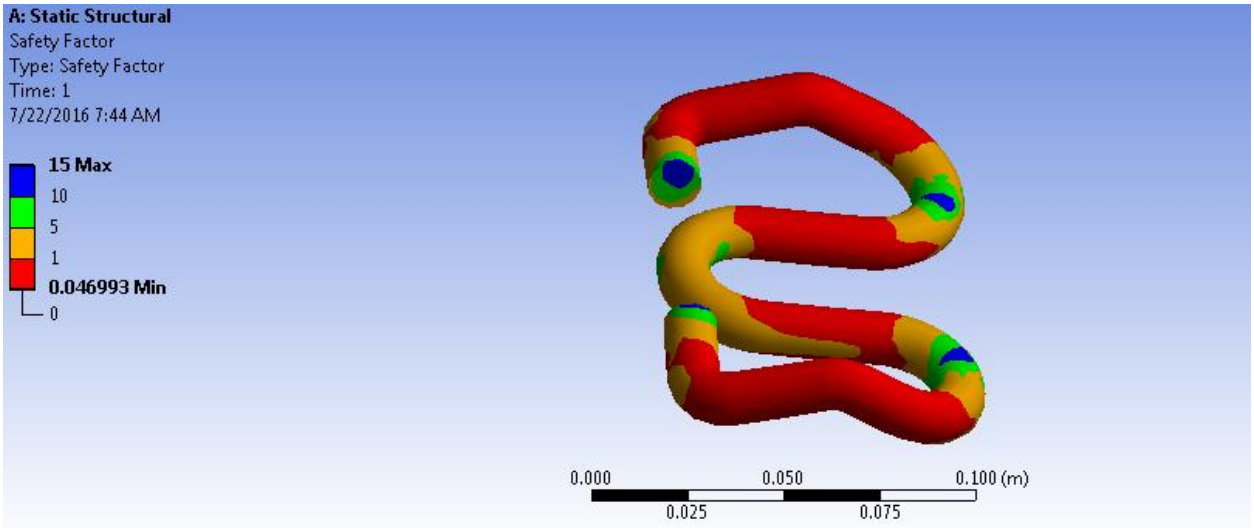

Figure 4.9: safety factor

As shown in above figure, the maximum safety factor is 15 and the minimum safety factor is 0.046993.

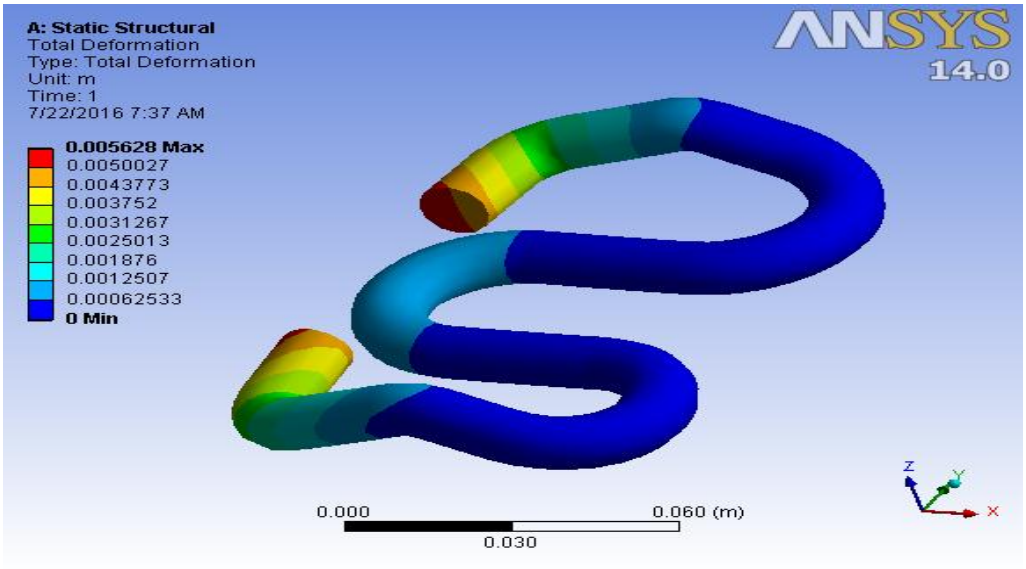

Figure 4.10.a. total deformation

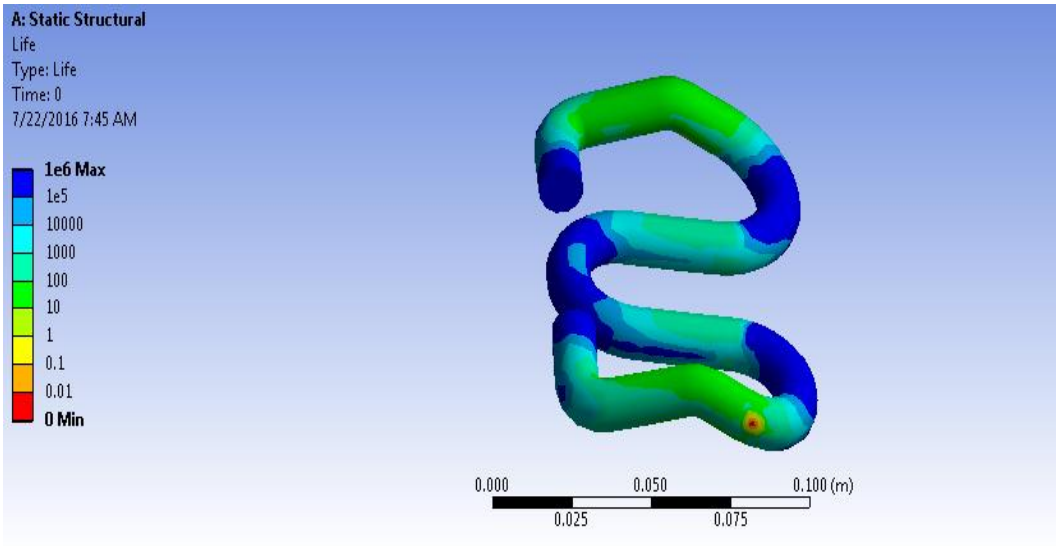

Figure 4.10.b. fatigue life

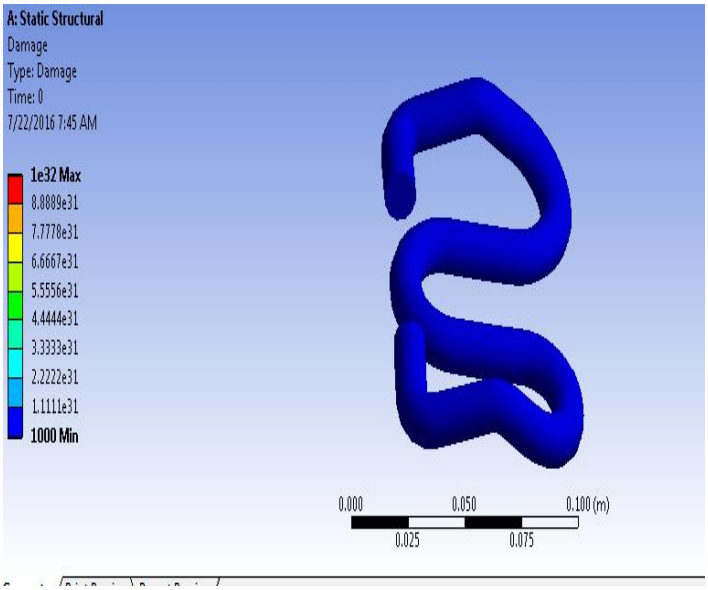

Figure 4.10.c. damage

Case 2: new geometry E-clamp

A- Alternating stress

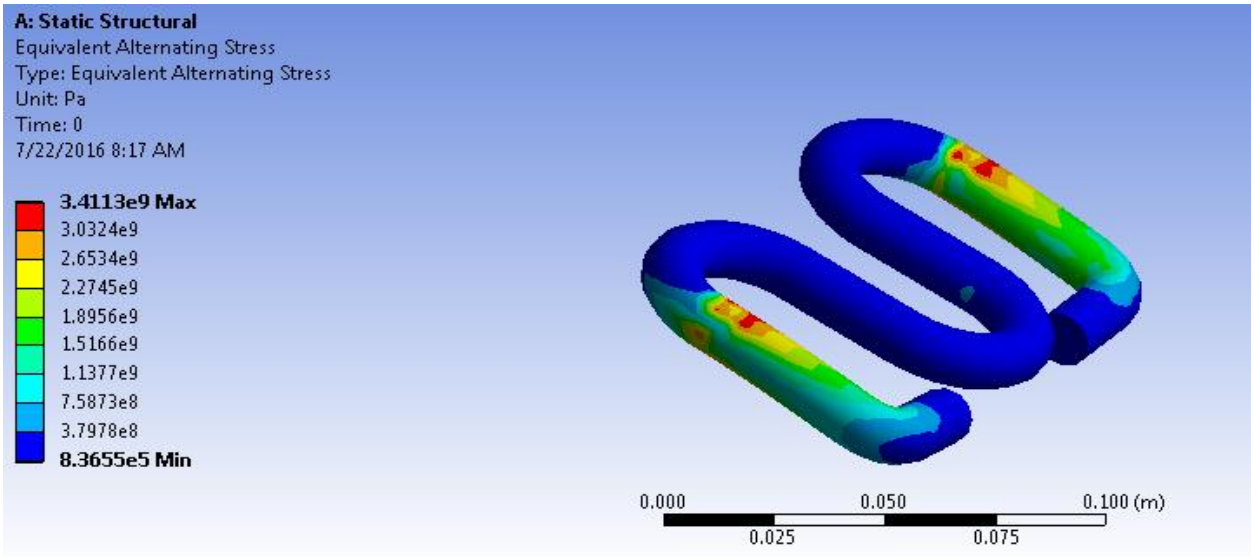

Figure 4.11: alternating stress

As shown in above figure, the maximum alternating stress is 3411.3MPa and the minimum alternating stress is 0.836MPa.

B-Biaxiality indication

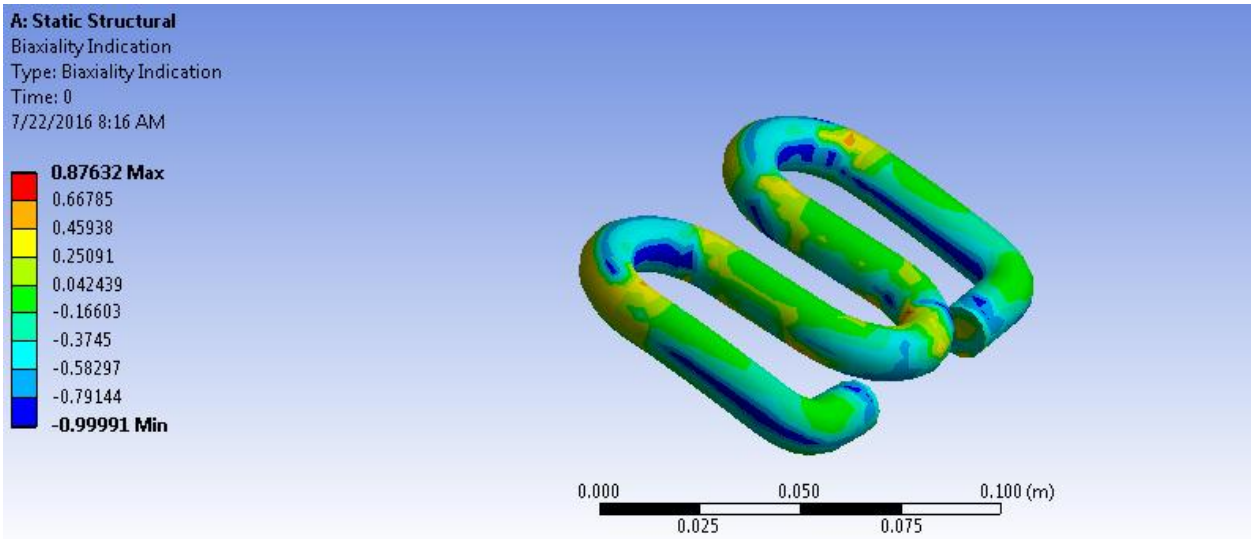

Figure 4.12.biaxiality indication

As shown in above figure, the maximum biaxial indication is 0.87632 and the minimum biaxial induction is -0.99991.

C-Factor of safety / fatigue life, damage and total deformation

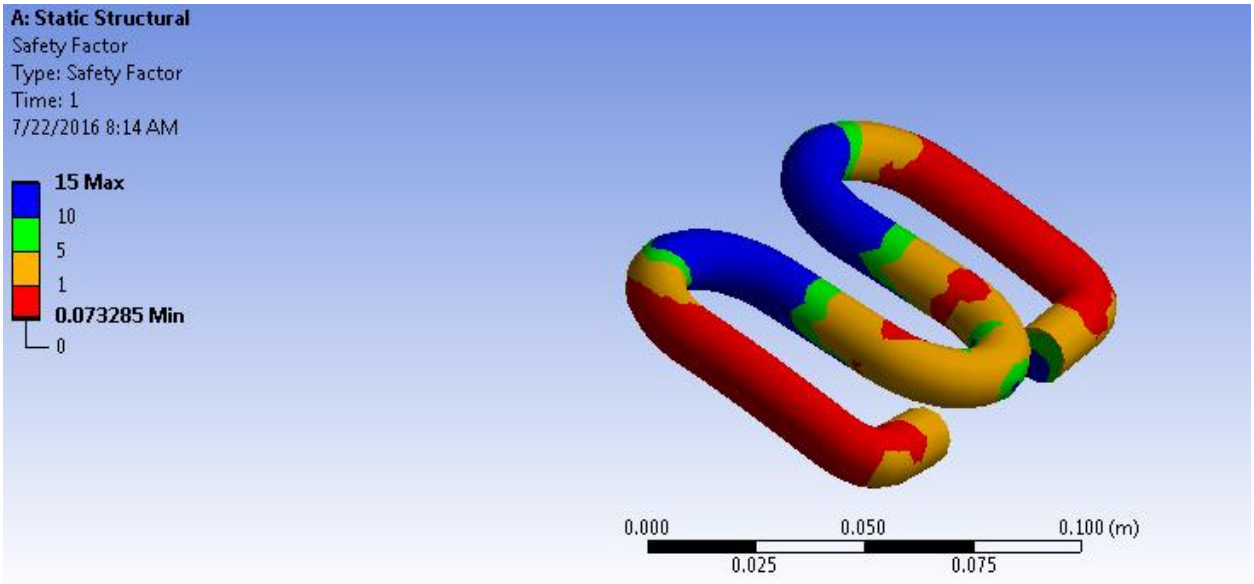

Figure 4.13. Safety factor

As shown in above figure, the maximum safety factor is 15 and the minimum safety factor is

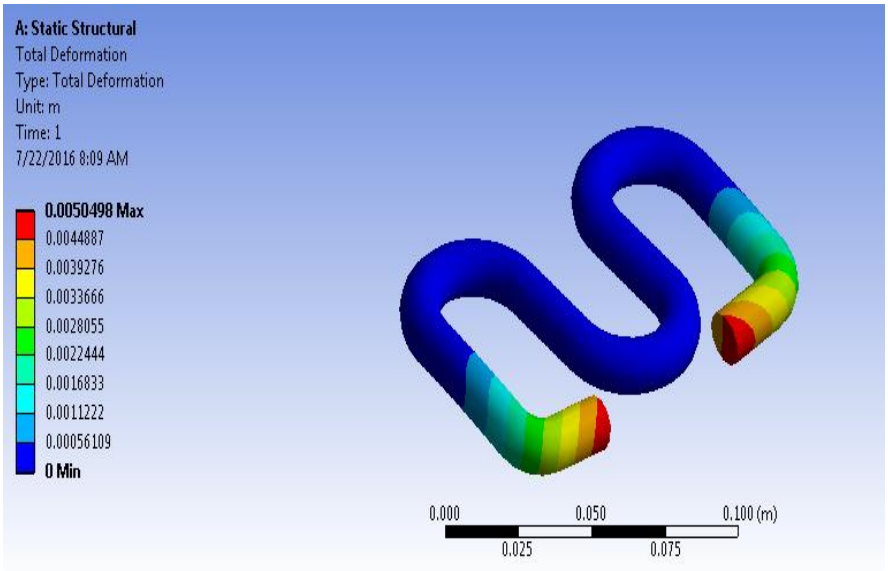

Figure 4.13.a. total deformation

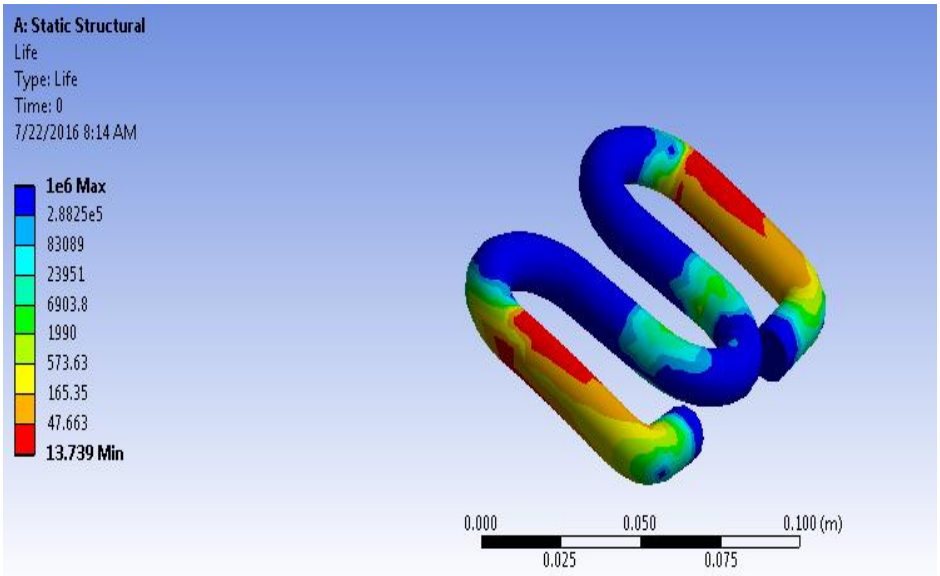

Figure 4.13.b. fatigue life

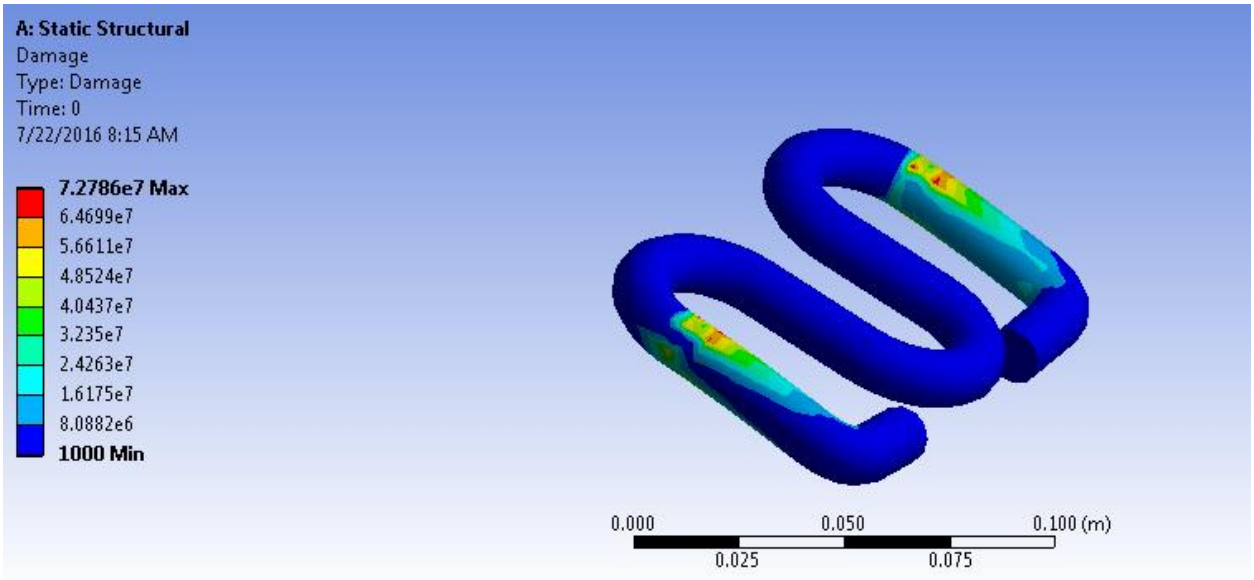

Figure 4.13.c. damage

4.2. Discussion

A three-dimensional finite element model is used to analysis the rail fastening section of track. The finite element program ansys is used to model the fastener analysis. This ANSYS is used to simulate the loading and boundary conditions of the rail and wheel contact for a stress analysis. This section of the paper specifies the result obtained from the ANSYS software based on hertz contact theory. The von miss stresses, maximum shear stress and Equivalent elastic strain have been determined under the influence of wheel load.

From literature [3] the maximum stress is 1200MPa is increasing according to time 6.68s.

From figure 4.14 the maximum stress is 5000MPa is increasing according to time 10s.

Table4.2: Static stress and fatigue analysis result summary [32]

Analysis type	Type of load		Case1 of the existing E-clamp	The new E-clamp
Static and fatigue analysis	Von-mises stress(MPa)	Max.	4714.6	3411.3
		Min.	4.611	0.836
	Normal stress(MPa)	Max.	3842.6	1466.2
		Min.	-2990.3	-1307.6
	Shear stress(MPa)	Max.	2267.6	1382.5
		Min.	-2355.3	-1382.4
	Safety factor	Max.	15	15
		Min.	0.046933	0.07
	Alternating stress (MPa)	Max.	4714.6	3411.3
		Min.	4.611	0.836

Case1: Existing E-clamp

Case2: new geometry E-clamp

The above result are included both E-clamp and wheel for the reason of the analysis performed using the contact mechanism. This paper mainly focuses on E-clamp part of rail fastening for that matter it ignores the wheel result.

As shown from static ANSYS result the value of the stress is vary for one case to other case. In case 1 as shown in the figure 4.2, 4.3 and 4.4 the maximum von mises, normal and shear stress

are 4714.6MPa, 3842.6MPa and 2267.6MPa on the existing E-clamp. In the case2 as shown in the figures 4.5, 4.6 and 4.7 the maximum von mises, normal and shear stresses are 3411.3MPa, 1466.2MPa and 1382.5MPa.

In comparision to yield strength, both stresses: the existing E-clamp and the new geometry are small. But the new geometry E-clamp stress is small as compared to the remaining E-clamp.

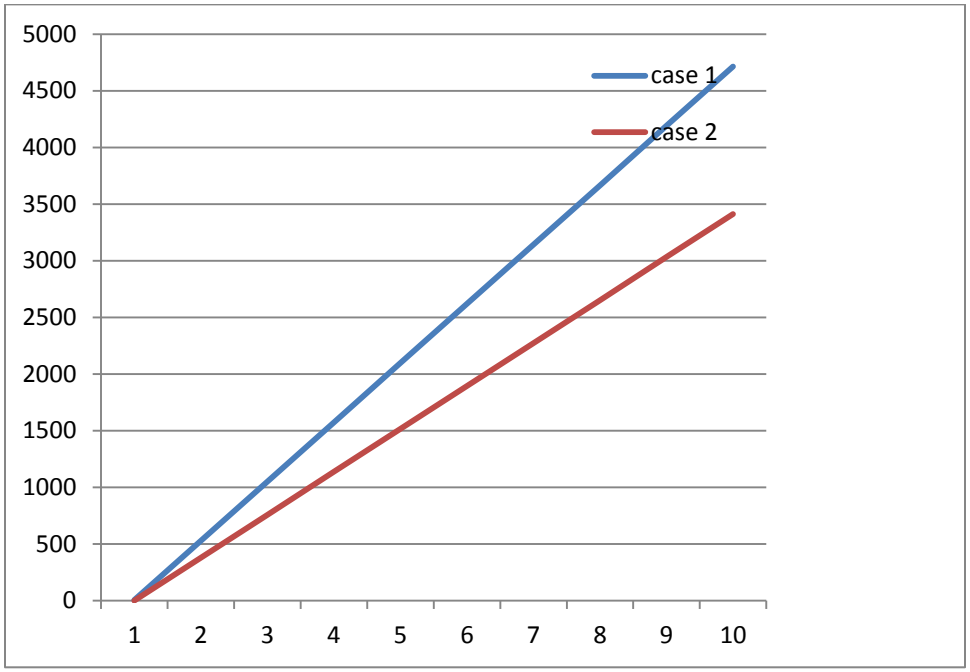

Figure 4.14: von-mises stress (MPa) graph versus time (10^-1s).

As shown in above figure, Von-Mises stress verses to time are given for two different geometry of E-clamp. The result shows that the von mises stress on rail fastening E-clamp increases with time. The von mises stress increases for two geometry of E-clamp. However, when compare two of them, for AA-LRT E-clamp stress distribution is highest than the other remaining new geometry E-clamp.

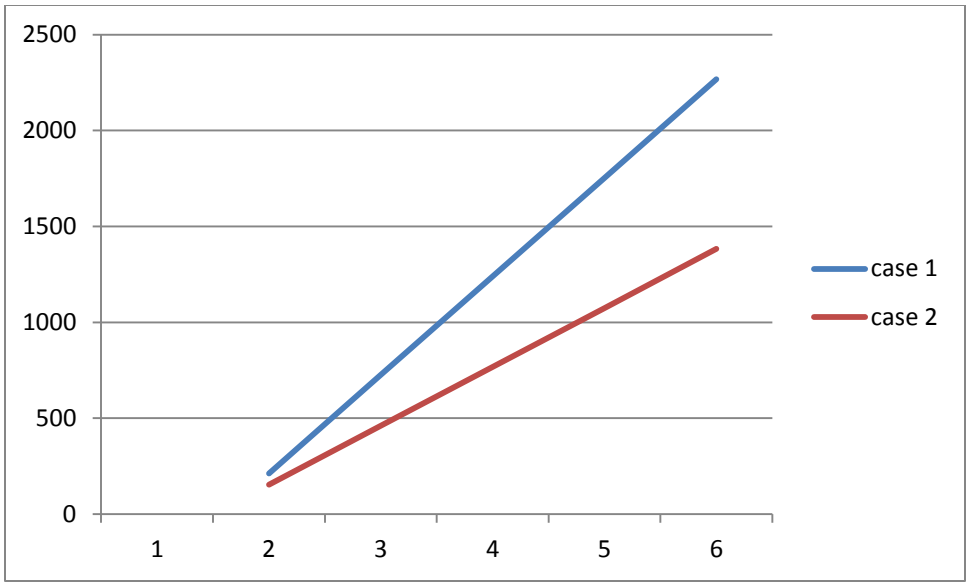

Figure 4.15: shear stress (MPa) graph versus time (0.1s).

As shown in above figure, the shear stress with time is given for two different geometry of E-clamp. The result shows that the shear stresses on E-clamp increases with increasing time. The shear stress increases for two different geometry of E-clamp. However, when compare two of them, AA-LRT E-clamp stress distribution is highest than the other remaining new geometry E-clamp.

In this paper fatigue analysis is used to check the failure of the E-clamp structure. From ANSYS result the three criteria are used to evaluate the failure of the

E-clamp, such as alternating stress, biaxial induction and safety factor.

Fatigue material properties are based on uniaxial stresses but real world stress states are usually multiaxial. Biaxiality indication is defined as the principal stress smaller in magnitude divided by the larger principal stress with the principal stress nearest zero ignored. A biaxiality of zero corresponds to uniaxial stress, a value of –1 corresponds to pure shear, and a value of 1 corresponds to a pure biaxial state.

Biaxiality indication of two cases are shown in Figures 4.8, and 4.12, pure shear and pure biaxial are exist in three cases.

Alternating stress are almost similar to the result obtain from von mises stress, so that it is not discuss detail.

Fatigue Life can be over the whole model or scoped just like any other contour result in Workbench. This result contour plot shows the available life for the given fatigue analysis. If

loading is of constant amplitude, this represents the number of cycles until the part will fail due to fatigue. If loading is non-constant, this represents the number of loading blocks until failure. Thus if the given load history represents one hour of loading and the life was found to be 24,000, the expected model life would be 1,000 days. In a Stress Life analysis with constant amplitude, if the equivalent alternating stress is lower than the lowest alternating stress defined in the S-N curve, the life at that point will be used. However when compare two of them, AA-LRT E-clamp minimum life cycle tolerate is 0 but the new geometry E-clamp is 13.739. It means the AA-LRT fatigue life is attend before any activities.

Fatigue Damage is a contour plot of the fatigue damage at a given design life. Fatigue damage is defined as the design life divided by the available life. This result may be scoped. For Fatigue Damage, values greater than 1 indicate failure before the design life is reached. Generally when compare the two materials we see that they are safe from failure before the design life is reached but the new geometry get some failure on its small part.

Fatigue Safety Factor is a contour plot of the factor of safety with respect to a fatigue failure at a given design life. The maximum Factor of Safety displayed is 15. Like damage and life, this result may be scoped. For Fatigue Safety Factor, values less than one indicate failure before the design life is reached. However when compare the two materials we observe that the AA-LRT E-clamp at its most part know the failure before the design life is reached because the value is less than 1.

The new geometry has the same composition of AA-LRT E-clamp and the contact between the new E-clamp and the sleeper is the same from AA-LRT E-clamp with rail clip and anchor and bolts with the same configuration but they differ from the geometry.

CHAPTER FIVE

5. CONCLUSION RECOMMENDATION AND FUTURE WORK

5.1 Conclusion

Relatively simple models of E-clamp were used for static analysis of the research. The prescribed method in this research may be used to estimate the fatigue life of E-clamp. The finite element model for reverse bending calculates E-clamp bending stresses that are comparable to the engineering estimates based on beam on elastic foundation.

In this study, the responses of a E-clamp component are determined under static, the results are assumed to be significant. The analysis can include stress, strain and fatigue responses of E-clamp caused by vertical wheel load. The stress value is reduced for the new geometry.

From the results obtained in the static and fatigue analysis, the two cases have different stress distribution. The stress distribution of AA-LRT E-clamp is high in comparison to new geometry E-clamp. The stress distribution of the new geometry E-clamp is small in comparison to the remaining the AA-LRT E-clamp.

5.2 Recommendation

This part of rail track needed more attention than other parts, to reduce the problem Related to the rail fastening. This paper recommends using the new E-clamp Geometry in comparision with the AA-LRT fastener. This paper is also Recommend, a material around the contact area between rail and E-clamp due to the exposure of the vertical load. In addition to this the E-clamp is seen in static and fatigue result, it is needed a special treatment to reduce the rail head wear Rate.

5.3 Future Work

In this paper the stress caused by vertical wheel load and some failure of rail fastening E-clamp are studied for different geometry of E-clamp. This paper studies mainly on finite element analysis, but to improve the problem related to the fastener, it is also needed field data to identify the exact place of failures and causes of failure.

The E-clamp needs more attention to eliminate problem related to the wheel/ rail contact like fracture of rail and looseness of nut and bolt or fracture of rail pad.

To minimize the E-clamp failure , the looseness of bolt and nut, and safety problem issues and maintenance cost of the railway track. It is also good to study and see more on following area:

- Stress-based fatigue on rail fastening spring clip
- Mechanisms behind rail seat deterioration
- Studying the failure cause of the rail pad

APPENDIX

1. Constant amplitude load:

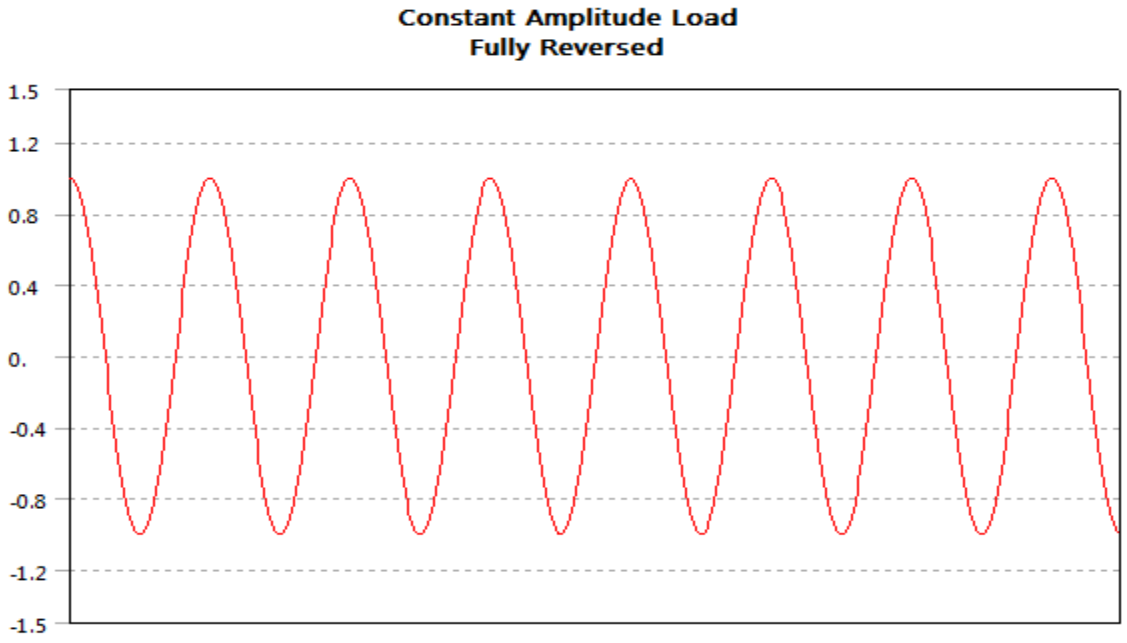

Figure 64: Constant load amplitude

2. Mean stress correction:

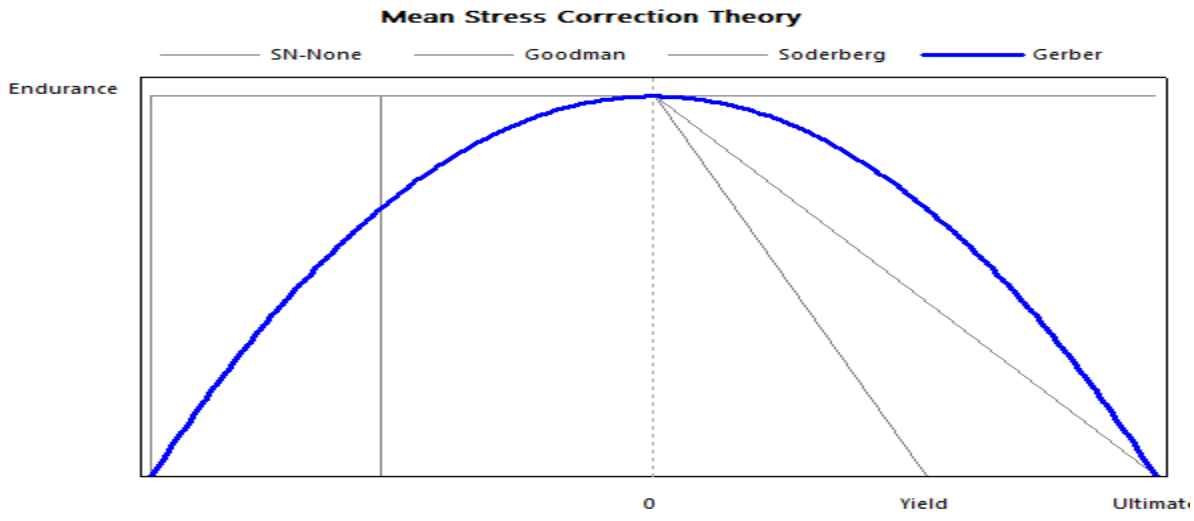

Figure 65: Mean stress correction theory

3. Idealized S-N Curve:

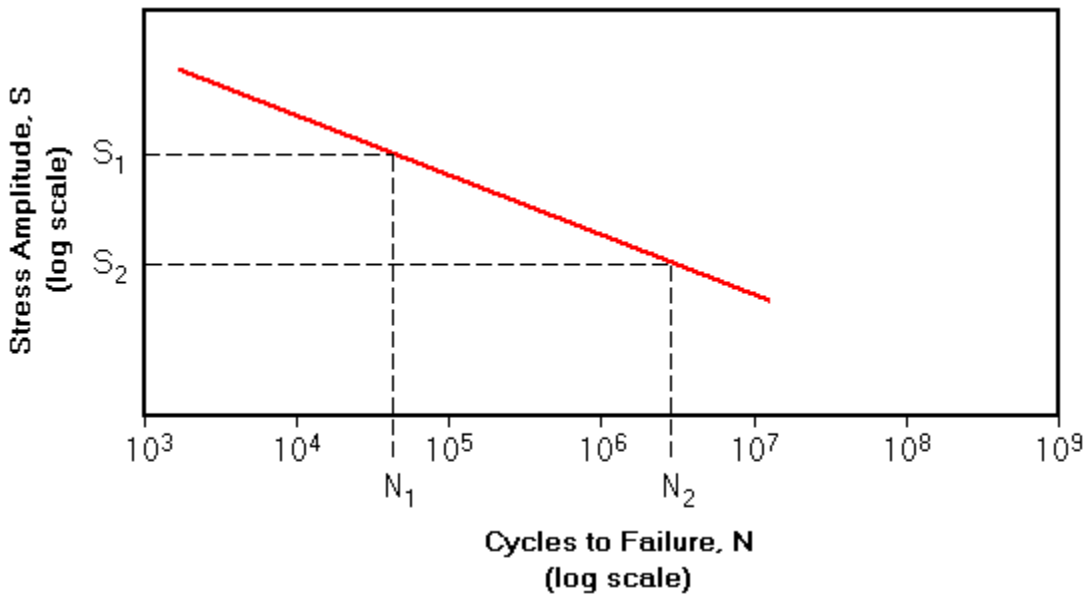

Figure 66: Idealized S-N Curve

4. Typical Cyclic Loading Parameters:

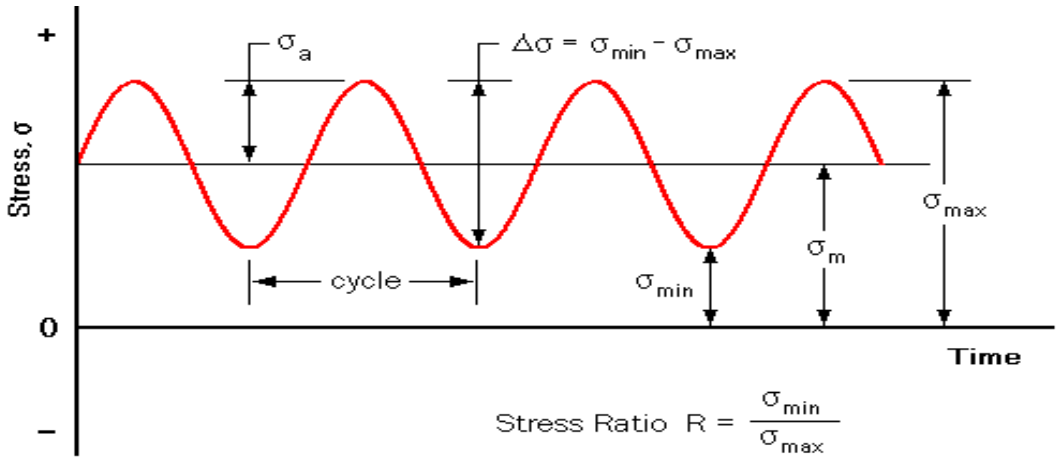

Figure 67: Typical Cyclic Loading Parameters

References

3. Kantantinos Giannokos: ‘’ Influences of the secondary stiffness of the rail fastening ‘’ 2001

4. Analysis of rail fastening system delta lager i failure ‘’analýza příčiny porušení upevňovacího systému kolejnic typu delta lager I’’Ing. Michal Mrózek, Ústav stavební mechaniky, Fakulta stavební, Vysoké, e-mail: mrozek.m@fce.vutbr.cz Ing. Petr Hradil, Ph.D., Ústav stavební mechaniky, Fakulta stavební, Vysoké e-mail: hradil.p@fce.vutbr.cz

5. ‘’ Stress-based Fatigue reliability analysis of rail fastening spring clip under traffic loads’ ’Saeed Mohammadzadeh/ / Sodayf Ahadi // Mehrdad Nouri 2007

6. ‘’Dynamic properties of railway track and its components : a state-of-the-art review’’ 2008 Sakdirat Kaewunruen Austrak Pty Ltd, sakdirat@uow.edu.au Alexander Remennikov University of Wollongong, alexrem@uow.edu.au

7.’’ New advances in Analysis and Design of railway track system’’ J. Sadeghi Iran University of Science and Technology, Iran

8.’’Transportation Engineering II ‘’ Dr Rajat Rastaji Indian Institute of Technology

9.’’ Types of rail fasteners ‘’ Dr Rastaji Indian Institute of Technology

10.’’ Railway Track component overview’’ New Advances in Analysis and Design of Railway Track System’’ J. Sadeghi Iran University of Science and Technology, Iran

11.’’ Lichtberger, B. Track compendium.’’(2007) Eurorailpress VA Profillidis. Railway management and engineering (2009) Asgathe.

12. W. Yan and F. D. Fischer ,Applicability of the Hertz contact theory to rail-wheel contact problems, Archive of Applied Mechanics 70 (2000) 255±268

13.’’ Pang, T. (2007) Studies on wheel/rail contact - impact forces at insulated rail joints’’, Master of Engineering Thesis, Centre for Railway Engineering, Central Queensland University, Australia

14. ‘’ Second Edition, National Academy of Sciences ,4-7-4-108.washington, d.c. W. Yan and F. D. Fischer ,Applicability of the Hertz contact theory to rail-wheel contact problems’’, Archive of Applied Mechanics 70 (2000) 255±268

15. ”Johnson, K. L. (1985) ,Contact Mechanics’’, (Cambridge University Press, Cambridge)

16. Jenkins, H. H.; Stephenson, J. E.; Clayton, G. A.; Morland, G. W.; and Lyon, D.

"The effect of track and vehicle parameters on wheel / rail vertical dynamic forces", Railway Engineering Journal, v3, n1, Jan, 1974, p 2-16.

17. Akhtar, M.N. and Davis, D.D. (2008) Preliminary results of prototype insulated joint tests at the Facility for Accelerated Service Testing, U.S. Department of Transportation, Federal Railroad Administration, RR08-11.

18. Peltier, D., Barkan, C.P.L., Downing, S., Socie D. (2007) Measuring degradation of bonded insulated rail joints, Proceedings of the AREMA 2007 Annual Conference, Chicago, IL, USA.